Irreversible Inactivation of Arylamine N-Acetyltransferases in the Presence of N-Hydroxy-4-Acetylaminobiphenyl: A Comparison of Human and Hamster Enzymes

ARTICLE *in* CHEMICAL RESEARCH IN TOXICOLOGY · MARCH 2005

Impact Factor: 3.53 · DOI: 10.1021/tx049801w · Source: PubMed

3 AUTHORS, INCLUDING:

Carston R Wagner
University of Minnesota Twin Cities
86 PUBLICATIONS **1,544** CITATIONS

SEE PROFILE

Irreversible Inactivation of Arylamine N-Acetyltransferases in the Presence of N-Hydroxy-4-Acetylaminobiphenyl: A Comparison of Human and Hamster Enzymes

Haiqing Wang,[†] Carston R. Wagner,[†] and Patrick E. Hanna*[,†,‡]

Departments of Medicinal Chemistry and Pharmacology, University of Minnesota, Minneapolis, Minnesota 55455

Received July 22, 2004

Arylamine N-acetyltransferases (NATs) catalyze the N-acetylation of arylamines, the O-acetylation of N-arylhydroxylamines, and the conversion of N-(aryl)acetohydroxamic acids to N-acetoxyarylamines. NATs also undergo irreversible inactivation in the presence of N-(aryl)-acetohydroxamic acids. We previously established that inactivation of hamster NAT1 by N-hydroxy-2-acetylaminofluorene is the result of sulfinamide adduct formation with Cys68. The purpose of this research was to determine the kinetics of inactivation of hamster NAT1, hamster NAT2, and human NAT1 by N-hydroxy-4-acetylaminobiphenyl (N-OH-4-AABP), to identify the amino acids that are modified upon NAT-catalyzed bioactivation of N-OH-4-AABP, to characterize the adducts and to identify factors that influence the propensity of NATs to undergo inactivation by N-arylhydroxamic acids. Mass spectrometric analysis of the NATs, after incubation with N-OH-4-AABP, revealed that the principal adduct of each protein was a (4-biphenyl)sulfinamide. Proteolysis of the adducted NATs caused hydrolysis of the sulfinamides to sulfinic acids. Tandem mass spectrometric analysis of the modified peptides revealed that each NAT isozyme contained a sulfinic acid on the Cys68 side chain. Minor adducts were identified as 4-aminobiphenyl conjugates of tyrosines. Hamster NAT1 was more rapidly inactivated by N-OH-4-AABP than either hamster NAT2 or human NAT1, and it was demonstrated that 4-nitrosoobiphenyl, which forms the sulfinamide adducts, accumulates during incubation of N-OH-4-AABP with hamster NAT2 and human NAT1 but not during incubations with hamster NAT1. Steady state kinetic analysis of the hydrolysis of acetylated NATs revealed that the half-lives of acetylated hamster NAT2 and human NAT1 are 7−8-fold greater than that of acetylated hamster NAT1. These results support the proposal that the mechanism of inactivation of NATs by N-OH-4-AABP involves initial deacetylation to produce N-OH-4-aminobiphenyl, which after oxidative conversion to 4-nitrosobiphenyl reacts with Cys68 to form a sulfinamide. The relatively short half-life of the acetylated form of hamster NAT1 contributes to its greater susceptibility to inactivation by N-OH-4-AABP.

Introduction

Exposure to arylamines, such as 4-aminobiphenyl (4-ABP),[1] is a recognized risk factor for human bladder cancer (*1*, *2*). Although exposure to carcinogenic arylamines occurs in certain occupational settings, the principal source of human exposure to 4-ABP is through inhalation of tobacco smoke and, possibly, through use of permanent hair dyes (*1*−*4*).

4-ABP is a genotoxic carcinogen, which undergoes metabolic conversion to electrophilic products that form covalent adducts with DNA (*5*). 4-ABP−DNA adduct levels in human breast and bladder tissue have been shown to be associated with the smoking of tobacco (*6*, *7*). Similar to other carcinogenic arylamines, the in vivo metabolism of 4-ABP includes its conversion to the arylhydroxamic acid, N-hydroxy-4-AABP (N-OH-4-AABP) (*8*, *9*). Bioactivation of either 4-ABP or its hydroxylamine (N-OH-4-ABP) and hydroxamic acid (N-OH-4-AABP) metabolites also results in the formation of protein adducts. Administration of N-OH-4-AABP to rats resulted in extensive covalent binding to liver protein, a portion of which was attributed to activation of the hydroxamic acid by conjugation with sulfate (*10*). N-Sulfonyloxy-N-acetyl-4-aminobiphenyl also was suggested to be the reactive metabolite responsible for the formation of a 4-acetylaminobiphenyl (4-AABP)−serum albumin adduct in rats treated with 4-ABP (*11*). Only a small percentage of protein adducts produced upon incubation of rat liver parenchymal cells with N-OH-4-

* To whom correspondence should be addressed. Tel: 612-625-4152. Fax: 612-624-0139. E-mail: hanna002@umn.edu.
[†] Department of Medicinal Chemistry.
[‡] Department of Pharmacology.

[1] Abbreviations: AAB, 4-aminoazobenzene; 4-AABP, 4-acetylaminobiphenyl; AcCoA, acetyl coenzyme A; 4-ABP, 4-aminobiphenyl; DEAE, dienthylaminoethyl; DHFR, dihydrofolate reductase; DMSO, dimethyl sulfoxide; DTT, dithiothreitol; EDTA, ethylenediaminetetraacetic acid; ESI, electrospray ionization; IPTG, isopropyl-D-thiogalactopyranoside; MALDI-TOF, matrix-assisted laser desorption/ionization time-of-flight; NAT, arylamine N-acetyltransferase; N-OH-4-ABP, N-hydroxy-4-ABP; N-OH-AAF, N-hydroxy-AAF; N-OH-4-AABP, N-hydroxy-4-AABP; PABA, *p*-aminobenzoic acid; PNPA, *p*-nitrophenylacetate; Q-TOF, quadrupole time-of-flight; rp, reverse phase; TFA, trifluoroacetic acid.

10.1021/tx049801w CCC: $30.25
Published on Web 00/00/0000 PAGE EST: 14.7

AABP retained the N-acetyl group of the hydroxamic acid, indicating that the N-acetyl group was enzymatically cleaved prior to the formation of electrophilic reactants or that it was lost during the bioactivation and adduct formation processes (*12*). Both the specific structures of the 4-ABP−protein adducts and the specific mechanism(s) of bioactivation responsible for protein adduction are unknown.

Arylamine N-acetyltransferases (NATs, EC 2.3.1.5) are polymorphic enzymes that catalyze the acetyl coenzyme A (AcCoA)-dependent N-acetylation of arylamines and O-acetylation of arylhydroxylamines, as well as the AcCoA-independent conversion of N-(aryl)acetohydroxamic acids, such as N-OH-4-AABP, to N-acetoxyarylamines (Ar-NH-$OCOCH_3$) (*13*). The latter products are relatively unstable molecules that undergo heterolytic cleavage of the N−O bond to yield arylnitrenium ions, which are believed to be the ultimate electrophilic reactants responsible for DNA adduct formation (*14*−*16*). We recently reported that the inactivation of hamster NAT1, which occurs during incubation with the carcinogenic arylhydroxamic acid, N-hydroxy-AAF (N-OH-AAF), results from the reaction of the side chain thiol group of the catalytically essential Cys68 with 2-nitrosofluorene, rather than through reaction with a 2-fluorenylnitrenium ion (*17*).

Humans and hamsters express two NAT genes, which exhibit deduced amino acid sequence identities of 69−82% (*18*). Although human NAT1 and hamster NAT2 have similar substrate selectivities and the substrate preferences of human NAT2 correspond to those of hamster NAT1, the capacity for conversion of arylhydroxamic acids, via N,O-acyltransfer, to DNA binding reactants is exhibited primarily by the NAT1 isozymes of both human and hamster (*19*, *20*). Consistent with the latter observation are the findings that hamster NAT1 is much more efficient than hamster NAT2 with regard to catalyzing the conversion of N-OH-AAF to products that lead to inactivation of the enzyme and that N-OH-4-AABP is an apparent mechanism-based inactivator of hamster NAT1 (*20*, *21*).

Hamsters are important models for study of the human acetylation polymorphism and for the investigation of the metabolism, bioactivation, and toxicity of arylamines and their metabolites (*22*, *23*). Thus, acquisition of an understanding of the similarities and differences in the interaction of these xenobiotics with human and hamster NATs is critical to the development of a basis for predicting the consequences of exposure to arylamines. Our development of a convenient protocol for overexpression and purification of human NAT1 made it possible to conduct kinetic comparisons of the inactivation of human NAT1 and hamster NAT1 and NAT2 by the carcinogenic arylhydroxamic acid, N-OH-4-AABP. The results of these studies are presented in this paper, along with the results of mass spectrometric analyses, which characterize the specific NAT adducts responsible for the loss of catalytic activity after activation of N-OH-4-AABP by the three NATs.

Experimental Procedures

Caution: *N-OH-4-AABP and 4-nitrosobiphenyl should be handled in accordance with NIH Guidelines for the Laboratory Use of Chemical Carcinogens (24).*

Materials and Methods. N-OH-4-AABP was synthesized as reported (*25*). Bio-Spin 6 Tris columns were purchased from Bio-Rad (Hercules, CA); anisidine, endopeptidase Glu-C, endopeptidase Lys-C, pepsin A, *p*-aminobenzoic acid (PABA) (sodium salt), *p*-nitrophenylacetate (PNPA), and trifluoroacetic acid (TFA) were purchased from Sigma (St. Louis, MO). *Escherichia coli* BL-21 Codon Plus RIL cells were purchased from Stratagene (La Jolla, CA). The reverse phase (rp) HPLC C4 (214MS54) and C18 (218MS21) columns were purchased from Vydac. All other reagents were purchased from Fisher Scientific, Inc. (Chicago, IL). Protein concentrations were determined by the method of Bradford (*26*). Spectrophotometric data were collected with a Varian Cary 50 UV−vis spectrophotometer. All rpHPLC was performed with a Beckman Coulter Gold system equipped with a diode array UV detector. All buffers were degassed under vacuum, and all incubations were conducted under aerobic conditions. The concentrations of all solutions given as percentages are v/v. Kinetic data were analyzed by JMP IN software suite (SAS Institute, Inc.), and statistical data were analyzed by ANOVA with SAS 8.0 software (SAS Institute, Inc.).

Synthesis of 4-Nitrosobiphenyl. A modification of reported methods was used (*27*, *28*). Pd/C (10%, 250 mg) was added to 4-nitrobiphenyl (1.8 g, 10 mmol) dissolved in tetrahydrofuran (250 mL) under argon. The solution was cooled to 0−2 °C with an ice water bath and stirred vigorously during the addition of hydrazine hydrate (99%, 2 mL). The formation of N-OH-4-ABP was monitored by TLC (silica gel, ethyl acetate:*n*-hexane; R_f, 0.1). After 2 h, the reaction mixture was filtered quickly through Celite, and ethyl acetate (50 mL) was added to the filtrate. The solution was washed with distilled water (3 × 100 mL), and the organic phase was dried over Na_2SO_4. The organic phase was then filtered, and the solvent was removed under vacuum. The residue (1 g) was dissolved in 40 mL of ethanol and was added dropwise, with stirring, to ferric chloride (5.5 equiv, 6 g) in 125 mL of ice water at 0−2 °C. After 30 min, the reaction mixture was filtered through Celite, dichloromethane (200 mL) was added to the filtrate, and the solution was extracted with distilled water (3 × 100 mL). The organic layer was dried with Na_2SO_4 and filtered, and the solvent was removed under reduced pressure. The crude product was purified by flash chromatography on silica gel (chloroform). The fractions containing the pure product were combined, and the solvent was removed under reduced pressure to afford 4-nitrosobiphenyl as a bright yellow powder: yield, 250 mg (25%); mp 72−74 °C (lit mp 73−74 °C). UV (methanol): λ_{max} 233 nm, 339 nm (lit λ_{max} 232 nm, 337 nm) (*29*, *30*).

Expression and Purification of Human Recombinant NAT1. The protocol for overexpression and purification of human recombinant NAT1 will be reported in detail elsewhere. Briefly, expression construct, pPH80D, containing the gene encoding human NAT1, was transformed to competent BL-21 Codon Plus RIL *E. coli* cells according to the supplier's instructions. The cells were grown at 37 °C to an A_{600nm} of 1.0 in LB medium containing ampicillin (100 μg/mL) and chloramphenicol (50 μg/mL). Isopropyl-D-thiogalactopyranoside (IPTG) (final concentration, 100 μM) was added to the culture after the culture had been quickly cooled to 30 °C. The growth was continued for 4 h at 30 °C. The cells were harvested by centrifugation at 5000*g* for 15 min at 4 °C. Cell lysis, partial purification of the mutant dihydrofolate reductase (DHFR)−human NAT1 fusion protein, thrombin cleavage of the fusion protein, and purification of the recombinant human NAT1 by diethylaminoethyl (DEAE)-sepharose chromatography were carried out by modifications of the procedures used previously for hamster NAT1 and NAT2 (*20*, *31*). The purified enzyme was homogeneous according to SDS−PAGE and electrospray ionization (ESI) quadrupole time-of-flight (Q-TOF) MS.

Expression and Purification of Hamster Recombinant NAT1 and NAT2. Hamster recombinant NAT1 and NAT2 were expressed and purified as described previously (*20*, *31*). Homogeneous hamster recombinant NAT1 and NAT2 were dialyzed into potassium phosphate buffer [20 mM, pH 7.4; 1 mM ethylenediaminetetraacetic acid (EDTA); 0.1 mM dithiothreitol

(DTT)]. Glycerol was added to a final concentration of 10%, and the proteins were stored at −80 °C.

Hamster NAT1 Activity Assay. The assay was carried out with PNPA as the acetyl donor and anisidine as the acetyl acceptor. The reaction rates were determined by monitoring the increase in absorbance at 400 nm due to the formation of *p*-nitrophenol (ϵ_{400nm} = 9400 M^{-1} cm^{-1}). Incubations were conducted at 25 °C in 1.5 mL acryl cuvetts with a Varian Cary 50 UV−vis spectrophotometer equipped with a circulating water bath. The reaction mixture contained hamster NAT1 (80 ng/mL, 23.4 nM), PNPA (2 mM), anisidine (1 mM), and MOPS buffer (100 mM, pH 7.0; 150 mM NaCl; 0.1 mM DTT) in a final volume of 500 μL. The transacetylation reaction was initiated by the addition of PNPA dissolved in dimethyl sulfoxide (DMSO) (5 μL). The nonenzymatic hydrolysis of PNPA was corrected by measuring the rate of the reaction in the absence of enzyme. The specific activity was expressed in units of μmol/mg of protein/min.

Human NAT1 and Hamster NAT2 Activity Assays. The assays were carried out as described for the hamster NAT1 activity assay, except the final concentration of the enzyme was 0.5 μg/mL (14.6 nM), and PABA, in a final concentration of 0.5 mM, was used as the acetyl acceptor.

Human NAT1 Activity Assay with N-OH-AAF/4-Aminoazobenzene (AAB). The assay was performed as described previously except the protein concentration was 16.2 μg/mL (473 nM) (*32*).

Time-Dependent Inactivation of Hamster NAT1 by N-OH-4-AABP at 37 °C. The incubation mixtures contained hamster NAT1 (8 μg/mL, 234 nM), N-OH-4-AABP (25−1000 μM), and tetrasodium pyrophosphate buffer (50 mM, pH 7.0; 0.1 mM DTT) in a total volume of 100 μL. The reaction was initiated by the addition of N-OH-4-AABP dissolved in DMSO (5 μL). The final concentration of DMSO was 1%. Aliquots (5 μL) were withdrawn at 30 s intervals (0−210 s) and transferred to an assay cuvett containing anisidine (1 mM) and MOPS buffer (100 mM; 150 mM NaCl, pH 7.0; 0.1 mM DTT). PNPA dissolved in DMSO (5 μL) was added to initiate the activity assay as described above. The percentage of activity remaining after incubation with N-OH-4-AABP was calculated with respect to the controls, which contained DMSO but not N-OH-4-AABP.

Time-Dependent Inactivation of Human NAT1 and Hamster NAT2 by N-OH-4-AABP at 37 °C. The incubation mixtures contained human NAT1 or hamster NAT2 (50 μg/mL, 1.46 μM), N-OH-4-AABP (100−1000 μM for human NAT1 and 100−800 μM for hamster NAT2), and tetrasodium pyrophosphate buffer (50 mM, pH 7.0, 0.1 mM DTT) in a total volume of 100 μL. The reaction was initiated by addition of N-OH-4-AABP dissolved in DMSO (5 μL). The final concentration of DMSO was 1%. Aliquots (5 μL) were withdrawn at 2 min intervals (0−12 min) and transferred to an assay cuvett containing PABA (0.5 mM) and MOPS buffer (100 mM, pH 7.0; 150 mM NaCl; 0.1 mM DTT). PNPA dissolved in DMSO (5 μL) was added to initiate the activity assay as described above. The percentage of activity remaining after incubation with N-OH-4-AABP was calculated with respect to the controls, which contained DMSO but not N-OH-4- AABP.

Inactivation of Hamster NAT1, Hamster NAT2, and Human NAT1 by 4-Nitrosobiphenyl. Incubation mixtures contained either hamster NAT1, hamster NAT2, or human NAT1 (25 μg/mL, 730 nM), 4-nitrosobiphenyl (0−10 μM), and potassium phosphate buffer (20 mM, pH7.4; 1 mM EDTA) in a total volume of 150 μL. Incubations were conducted at 23 °C. The reaction was initiated by addition of 4-nitrosobiphenyl dissolved in DMSO (3 μL). The final concentration of DMSO was 2%. After a 1 min incubation, 2 μL of reaction mixture was removed for NAT activity assays.

Half-Lives of Acetyl-Enzyme Intermediates. In a final reaction volume of 400 μL, hamster NAT1 (1.67 μM), hamster NAT2 (1.96 μM), or human NAT1 (1.04 μM) was incubated with PNPA (2 mM) in MOPS buffer (100 mM, pH 7.0; 150 mM NaCl; 0.1 mM DTT) at either 25 or 37 °C. The reactions were initiated by addition of PNPA dissolved in DMSO (2 μL) and were monitored continuously at 400 nm for 5 min. The final concentration of DMSO was 0.5%. The rates of acetyl−enzyme intermediate hydrolysis were determined as the increase in absorbance at A_{400nm} (ϵ_{400nm} = 9400 M^{-1} cm^{-1}) due to the formation of *p*-nitrophenol. Control experiments were conducted in which the enzymes were omitted.

Formation of 4-Nitrosobiphenyl from N-OH-4-AABP in the Presence of NATs. In a final volume of 500 μL, hamster NAT1, hamster NAT2, or human NAT1 (4 μM) was incubated with N−OH-4-AABP (200 μM) in MOPS buffer (100 mM, pH 7.0; 150 mM NaCl; 0.025 mM DTT) at 37 °C for 30 min. The buffer was extensively degassed under vacuum and purged with argon before use, and more than 95% control NAT activities were retained after a 30 min incubation at 37 °C. The reactions were initiated by addition of N-OH-4-AABP dissolved in DMSO (4 μL). The final concentration of DMSO was 0.8%. Formation of 4-nitrosobiphenyl was monitored continuously at A_{350nm} (ϵ_{350nm} = 11800 M^{-1} cm^{-1}). Control experiments were conducted in which the enzymes were omitted.

Sample Preparation for ESI-Q-TOF MS of N-OH-4-AABP-Treated Hamster NAT1. To hamster NAT1 (114 μg, 43.5 μM) in potassium phosphate buffer (76 μL, 20 mM, pH 7.4; 1 mM EDTA; 10% glycerol; 0.1 mM DTT) was added N-OH-4-AABP dissolved in 4 μL of DMSO. The final concentration of N-OH-4-AABP was 500 μM. DMSO only was added to the control incubation mixtures. The mixture was incubated for 5 min at 23 °C, which resulted in more than 90% loss of activity. The reaction was terminated by loading the reaction mixture onto a Bio Spin 6 Tris column, which had been equilibrated with the potassium phosphate buffer. After centrifugation at 1000*g* for 4 min, 8 μL of the solution was used to measure the protein concentration and residual hamster NAT1 activity. To the remaining solution, 16 μL of acetic acid (10%) and 1 μL of TFA (1%) were added to adjust the pH to 3.0. The sample was centrifuged at 16000*g* for 5 min at 4 °C, and the supernatant was subjected to rpHPLC on a Vydac C4 MS column (214MS54, 4.6 mm × 250 mm). A stepwise isocratic elution with a flow rate of 1 mL/min was used. Solvent A was 2.5% acetonitrile with 0.01% TFA, and solvent B was 95% acetonitrile with 0.01% TFA. The column was eluted with 0% B (2 min), 40% B (4 min), 60% B (7 min), and 100% B (5 min). The elution profile was recorded at both 220 and 280 nm. Hamster NAT1 eluted at 10.2 min. The protein-containing fractions were stored at −80 °C.

Sample Preparation for ESI-Q-TOF MS of 4-Nitrosobiphenyl-Treated Hamster NAT1. To hamster NAT1 (114 μg, 43.5 μM) in potassium phosphate buffer (76 μL, 20 mM, pH 7.4; 1 mM EDTA; 10% glycerol; 0.1 mM DTT) was added 4-nitrosobiphenyl dissolved in 4 μL of DMSO. The final concentration of 4-nitrosobiphenyl was 250 μM. DMSO only was added to the control incubation mixtures. The mixture was incubated for either 5 or 10 min at 23 °C, which resulted in greater than 95% loss of activity. The reactions were terminated, and the protein was prepared for MS analysis as described above for N-OH-4-AABP-treated hamster NAT1.

Sample Preparation for ESI-Q-TOF MS of N-OH-4-AABP-Treated and 4-Nitrosobiphenyl-Treated Hamster NAT2. The experimental procedure was the same as described for N-OH-4-AABP-treated and 4-nitrosobiphenyl-treated hamster NAT1, except the incubation time for hamster NAT2 with N-OH-4-AABP was 15 min, and with 4-nitrosobiphenyl it was 10 min.

Sample Preparation for Nano-ESI-Q-TOF MS of N-OH-4-AABP-Treated Human NAT1. To human NAT1 (38 μg, 29 μM) in potassium phosphate buffer (38 μL, 20 mM, pH 7.4; 1 mM EDTA; 10% glycerol; 0.1 mM DTT) was added N-OH-4-AABP dissolved in 2 μL of DMSO. The final concentration of N-OH-4-AABP was 500 μM. DMSO only was added to the control incubation mixtures. The incubations were conducted at 23 °C. After 15 min, a portion (8 μL) of the reaction mixture was used to measure the residual activity, which was less than 10% of the control activity. The reaction was stopped by

immersion in a dry ice−acetone bath, and a 3 μL portion of the sample was used for nanoelectrospray MS. A control incubation, to which DMSO had been added rather than N-OH-4-AABP, was carried out by an identical procedure.

Sample Preparation for Nano-ESI-Q-TOF MS of 4-Nitrosobiphenyl-Treated Human NAT1. The experimental procedure was the same as described for N-OH-4-AABP-treated human NAT1 except that the incubation times for human NAT1 with 4-nitrosobiphenyl were 5 and 10 min, and the 4-nitrosobiphenyl concentration was 250 μM.

Pepsin Digestion of N-OH-4-AABP-Treated Hamster NAT1, Hamster NAT2, and Human NAT1. Hamster NAT1, hamster NAT2, and human NAT1 were inactivated with N-OH-4-AABP under conditions identical with those described above for the sample preparation for ESI-Q-TOF MS. The reactions were terminated by loading the reaction mixtures onto Bio Spin 6 Tris columns, which had been equilibrated with tetrasodium pyrophosphate buffer (5 mM, pH 7.0; 0.1 mM DTT). After centrifugation at 1000*g* for 4 min, 8 μL of the solution was used to measure the protein concentration and residual NAT activity. To 70 μL of the remaining solution, 5 μL of 1 N HCl was added to adjust the pH to 1.3. Digestion was initiated by addition of pepsin (1 mg/mL in H_2O, pH 1.3). The ratio of pepsin to each NAT protein was approximately 1:100. After incubation at 37 °C for 3 h, the reaction was terminated by adjusting the pH to 8 with 1 N NaOH (4 μL). Acetonitrile (5 μL) was added, and the sample was stored at −80 °C for matrix-assisted laser desorption/ionization time-of-flight (MALDI-TOF) MS peptide mapping and sequencing. Control digests, to which DMSO had been added instead of the N-OH-4-AABP-DMSO solution, were obtained with the same procedure.

Pepsin Digestion of 4-Nitrosobiphenyl-Treated Hamster NAT1 and Human NAT1. Hamster NAT1 and human NAT1 were inactivated with 4-nitrosobiphenyl under conditions identical with those described above for the sample preparation for ESI-Q-TOF MS. The digestion procedures were identical to those described for pepsin digestion of N-OH-4-AABP-treated hamster NAT1 and human NAT1.

Pepsin Digestion of 4-Nitrosobiphenyl-Treated Hamster NAT2. Hamster NAT2 was inactivated with 4-nitrosobiphenyl under conditions identical with those described above for the sample preparation for ESI-Q-TOF MS. The digestion procedures were identical to those described for pepsin digestion of N-OH-4-AABP-treated hamster NAT2. To the digested sample, 1 μL of TFA (1%) was added to adjust the pH to 3.0, followed by centrifugation at 16000*g* for 5 min at 4 °C. The peptides were fractionated by rpHPLC on a Vydac C18 MS column (218MS21, 2.1 mm × 250 mm) at a flow rate of 0.2 mL/min. Solvent A was 5% acetonitrile in 0.01% TFA. Solvent B was 90% acetonitrile in 0.01% TFA. A stepwise gradient was used as follows: 0% B (0−5 min), 0−40% B (5−65 min), 40−70% B (65−95 min), and 70−100% B (95−115 min). The fractions were monitored at 220 and 280 nm and were collected at 1 min intervals. The peptide-containing fractions were screened and sequenced by MALDI-TOF MS. A control digest, to which DMSO had been added rather than 4-nitrosobiphenyl, was obtained in an identical fashion.

Endopeptidase Lys-C Digestion of Modified Peptide DQIVRKKRGGWCLQVNHLLY. The volume of the rpHPLC fraction containing the peptide (∼ 200 μL) was reduced to about 50 μL by centrifugation under vacuum with heating (37 °C). The pH of the solution was adjusted to ∼8.5 by adding 11 μL of ammonium bicarbonate buffer (1 M, pH 8.0). The digestion was initiated by adding 0.1 μg of endopeptidase Lys-C in water (1 μL). After a 4 h incubation at 37 °C, the digestion was terminated by acidification to pH ∼2−3 with 1% TFA, followed by addition of acetonitrile (5 μL). The samples were stored at −80 °C for MALDI-TOF MS peptide mapping and sequencing.

Endopeptidase Glu-C Digestion of N-OH-4-AABP-Treated and 4-Nitrosobiphenyl-Treated Hamster NAT1, Hamster NAT2, and Human NAT1. Hamster NAT1, hamster NAT2, and human NAT1 were inactivated with N-OH-4-AABP and 4-nitrosobiphenyl under conditions identical with those described above for the sample preparation for ESI-Q-TOF MS. Digestion was initiated by addition of endopeptidase Glu-C (2.5 mg/mL in H_2O, 2 μL). The ratio of endopeptidase Glu-C to each NAT protein was approximately 1:20. After incubation at 37 °C for 18 h, acetonitrile (5 μL) was added and the samples were stored at − 80 °C for MALDI-TOF MS peptide mapping and sequencing. Control digests were obtained with enzymes that had been incubated with DMSO, rather than N-OH-4-AABP dissolved in DMSO.

ESI-Q-TOF MS of Unmodified and Modified Hamster NAT1 and NAT2. Protein masses were obtained by direct infusion with a QSTAR Pulsar *i* Q-TOF from Applied Biosystems, Inc. (ABI, Foster City, CA). The IonSpray source was used with an ESI infusion flow rate of 25 μL/min (acetonitrile:water, 65:35, 0.01% TFA). The ESI voltage was 5000 V; mass spectra were the average of 300−600 scans collected in the positive ion mode. The TOF region acceleration voltage was 4 kV. The injection pulse repetition rate was 6.0 kHz. The series of multiply charged protein peaks from 700 to 3000 *m/z* were deconvoluted to provide protein zero-charge mass with the Bayesian Reconstruct tool in the ABI BioAnalyst software package.

Nano-ESI-Q-TOF MS of Unmodified and Modified Human NAT1. Human NAT1 samples were desalted with 20 μm Poros R2 resin (polystyrene divinylbenzene, ABI) in a glass purification capillary. The sample was loaded onto the R2 resin, washed three times with ∼7 μL of 5% acetonitrile−0.5% formic acid, and eluted into a coated nanoelectrospray capillary with ∼1.5 μL of 70% acetonitrile−0.5% formic acid. ESI mass spectra were acquired with a QSTAR Pulsar I Q-TOF mass spectrometer equipped with a nano-ESI source (Protana Engineering). The ESI voltage was 1000 V; the TOF region acceleration voltage was 4 kV; and the injection pulse repetition rate was 6.0 kHz. Mass spectra were the average of approximately 300 scans collected in a positive mode over a 5 min acquisition period. The series of multiply charged protein peaks from 700 to 3000 *m/z* were deconvoluted to provide protein zero-charge mass with the Bayesian Reconstruct tool in the ABI BioAnalyst software package.

MALDI-TOF MS Screening and Sequencing of Peptides. Prior to MALDI-TOF analysis, a portion of the digest was desalted with Millipore C18 ZipTips according to the protocol described by Millipore for peptides in solution with a high concentration of salt. Peptides in HPLC fractions were directly applied onto the target without an additional desalting step. Full scan mass spectra from *m/z* 600 to 3500 of the peptide mixtures were collected in the positive mode by averaging 100−300 spectra. Data were acquired on one of the following spectrometers: Bruker Biflex III (Bruker Daltonics, Bilerica, MA) mass spectrometer; Qstar pulsar *i* quadrupole-TOF mass spectrometer (ABI), or QSTAR XL quadrupole-TOF mass spectrometer (ABI). The Bruker Biflex III mass spectrometer is equipped with an N_2 laser (337 nm, pulse length of 3 ns). The full scan spectra were collected in the reflectron mode, with an accelerating potential of 19 kV with α-cyano-4-hydroxycinnamic acid (cca) (Agilent Technologies, Palo Alto, CA) as the matrix. For QSTAR XL MS, full scan and tandem mass spectra of selected ions were collected with cca as the matrix. The TOF region acceleration voltage was 4 kV, and the injection pulse repetition rate was 6.0 kHz. Laser pulses were generated with a nitrogen laser at 337 nm, with ∼9 μJ of laser energy, and with a laser repetition of 20 Hz. For Qstar Pulsar *i* MS, full scan and tandem mass spectra were collected with 2,5-dihydroxybenzoic acid (Agilent Technologies) as the matrix. The TOF region acceleration voltage was 4 kV, and the injection pulse repetition rate was 6.0 kHz. Laser pulses were generated with a nitrogen laser at 337 nm, with 33 μJ of laser energy, and with a laser repetition rate of 20 Hz. External calibration was performed with human angiotensin II (monoisotopic [MH^+], *m/z* 1046.5417; Sigma), angiotensin I (monoisotopic [MH^+], *m/z* 1296.6853; Sigma), and adrenocorticotropin hormone fragment

18−39 (monoisotopic [MH^+], *m/z* 2465.1989; Sigma).

MS Data Analysis. Theoretical masses of proteins, peptides, and fragment ions were generated with Protein Prosepector (http://prospector.ucsf.edu) and with the AS software package (ABI).

Results

Inactivation of Hamster NAT1, Hamster NAT2, and Human NAT1 by N-OH-4-AABP. Incubation of hamster NAT1, hamster NAT2, and human NAT1 with N-OH-4-AABP resulted in a time-dependent, concentration-dependent, and irreversible loss of enzyme activity. The rate of inactivation of hamster NAT1 was concentration-dependent at the lower concentrations of N-OH-4-AABP but was saturable at higher concentrations, indicating involvement of the enzyme's active site (data not shown). Linear semilog plots of percent remaining hamster NAT1 activity vs time were obtained with several concentrations of N-OH-4-AABP, and a first-order inactivation rate constant (k_{obs}) for each concentration was determined from the slopes of the lines (Figure 1a). An inactivation rate constant of 0.013 s^{-1} (k_i) and a dissociation constant of 202 μM (K_I) were obtained from a double reciprocal plot ($R^2 = 0.99$) of k_{obs} values vs N-OH-4-AABP concentrations (*33*). The second-order rate constant (k_i/K_I) for the inactivation of hamster NAT1 by N-OH-4-AABP is 64.4 M^{-1} s^{-1}. The values of the kinetic parameters obtained in these experiments with homogeneous recombinant enzyme are consistent with the previously reported k_i of 0.007 s^{-1} and K_I of 430 μM for inactivation of partially purified hamster hepatic NAT1 by N-OH-4-AABP (*21*).

In contrast to the results obtained with hamster NAT1, treatment of hamster NAT2 with N-OH-4-AABP did not result in an inactivation process that exhibited apparent first-order kinetics. Rather, the rate of inactivation of hamster NAT2 at longer incubation times was faster than that observed during shorter incubation periods (Figure 1b). For example, a 6 min incubation of hamster NAT2 with N-OH-4-AABP (400 μM) resulted in a 28% loss of activity, wheras after a 12 min incubation, 84% of the enzyme activity had been lost. The data shown in Figure 1b suggest that an accumulation of the inactivating reactant occurs during the initial phase of the incubation, followed by a more rapid rate of enzyme inactivation.

As shown in Figure 1c, little loss of human NAT1 activity occurs during the first 2 min of incubation with N-OH-4-AABP. After 2 min, however, the inactivation proceeds according to an apparent first-order process. A double reciprocal plot ($R^2 = 0.99$) of the k_{obs} values, derived from the slopes of the lines in Figure 1c, allowed the calculation of a k_i of 0.01 s^{-1} and a dissociation constant (K_I) of 1.26 mM for the inactivation of human NAT1 by N-OH-4-AABP (33). The second-order rate constant (k_i/K_I) is 7.9 M^{-1} s^{-1}. Thus, the k_i value for inactivation of hamster NAT1 by N-OH-4-AABP is approximately 1.5-fold greater than the corresponding value for inactivation of human NAT1, and the K_I for inactivation of hamster NAT1 is approximately 6-fold smaller than that the K_I for inactivation of human NAT1. The comparative second-order rate constants (k_i/K_I) indicate that hamster NAT1 is approximately 10-fold more susceptible than human NAT1 to inactivation by N-OH-4-AABP.

The data presented in Figure 1c suggest that an initial accumulation of inactivating reactant occurs prior to the onset of inactivation of human NAT1, as was observed for the inactivation of hamster NAT2 (Figure 1b). Furthermore, similar concentrations of N-OH-4-AABP caused similar losses of activity by hamster NAT2 and human NAT1 after 10−12 min incubations. For example, hamster NAT2 and human NAT1 incurred 49 and 53% losses in activity, respectively, in the presence of N-OH-4-AABP (200 μM),whereas a 400 μM concentration of the hydroxamic acid caused 76% inactivation of human NAT1 and an 84% decrease in hamster NAT2 activity.

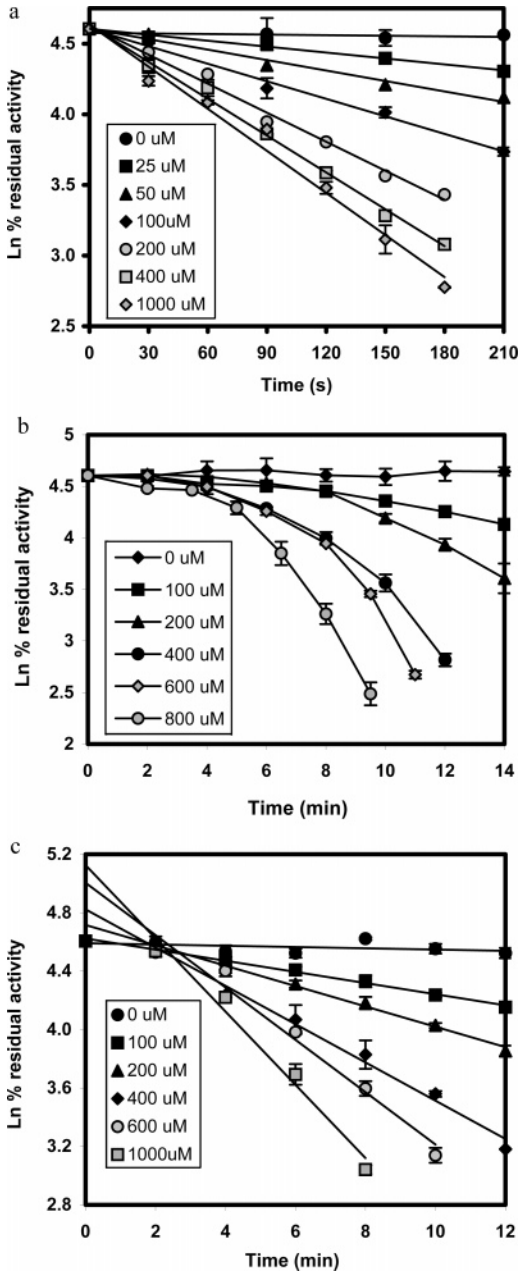

Figure 1. Time- and concentration-dependent inactivation of NAT activities by N-OH-4-AABP. (a) Hamster NAT1, (b) hamster NAT2, and (c) human NAT1. The results represent the means ± SD of three experiments. For some data points, the SD is smaller than the size of the symbol.

ESI Q-TOF Analysis of N-OH-4-AABP-Treated Hamster NAT1. On the basis of the results of our previous investigation of the inactivation of hamster NAT1 by N-OH-AAF, it was anticipated that the principal adducts formed as a result of treatment of NATs with N-OH-4-AABP would be (4-biphenyl)sulfinamides

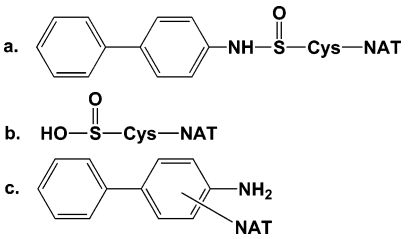

Figure 2. (a) (4-Biphenyl)sulfinamide−NAT adduct, (b) sulfinic acid−NAT modification, and (c) 4-ABP−NAT adduct.

(Figure 2a), which result from the reaction of 4-nitrosobiphenyl with the thiol groups of cysteine residues (*17*). It was also expected that minor adducts with 4-ABP would be produced (Figure 2c). The (4-biphenyl)sulfinamides and 4-ABP adducts would result in mass enhancements of 183 and 167 Da, respectively. Proteins were prepared for mass spectrometric analysis according to the conditions of our published protocol, which permits analysis of intact Cys68-sulfinamide-adducted NATs (*17*).

Native (unmodified) hamster NAT1 exhibited a molecular mass of 33903.0 Da, which closely matches the theoretical mass of 33900 Da, including the four additional amino acids (Gly, Thr, Gln, and Leu) that are present at the N terminus of the recombinant protein (Figure 3a). The mass spectrum of hamster NAT1 that had been treated with N-OH-4-AABP contained seven peaks, including the peak at 33895.1 Da, which corresponds to native hamster NAT1 (Figure 3b). The peak at 34078.2 Da is the result of the addition of 183 Da to the native protein and is consistent with formation of a sulfinamide adduct. The small peak at 34264.1 Da represents a mass increment of 186 Da to the 34078.2 Da peak and is consistent with the formation of a second sulfinamide adduct. The peak at 34421.3 Da is a result of a mass increase of 157 Da, relative to the 34264.1 Da peak. The mass of 157 Da is 10 Da less than the expected mass increment for a 4-ABP adduct (theoretical increase, 167 Da). The major peak of 34604.7 Da is consistent with addition of a sulfinamide adduct (183 Da) to the 34421.3 Da peak. Finally, the two minor peaks of 34767.1 and 34945.9 Da are the result of incremental additions of 162 and 178 Da, respectively, and may indicate the presence of a 4-ABP adduct and another (4-biphenyl)sulfinamide adduct.

Proteolysis of N-OH-4-AABP-Treated Hamster NAT1 and MALDI Q-TOF MS/MS. Previous reports from our laboratory have established that pepsin digestion of hamster NAT1 and NAT2 provides relatively complete coverage of the sequences and permits detection of modifications of the catalytically essential Cys68 (*17*, *34*, *35*). Thus, both native hamster NAT1 and N-OH-4-AABP-inactivated hamster NAT1 were subjected to treatment with pepsin. A manual comparison of the MALDI-TOF mass spectra of the peptides present in the digests revealed only one modified peptide (monoisotopic mass, 2458.32 Da) (Supporting Information, Figure S1). Furthermore, a peptide of monoisotopic mass 2426.32 Da, corresponding to the peptide sequence of DQIVRKKRGGWCLQVNHLLY (Asp57−Tyr 76; unmodified theoretical mass 2426.32 Da) was present in the control digest but not in the pepsin digest of N-OH-4-AABP-inactivated hamster NAT1.

The modified peptide of mass 2458.32 was subjected to MALDI Q-TOF MS/MS analysis. The tandem mass data shown in Figure 4 indicate a modified (+32 Da)

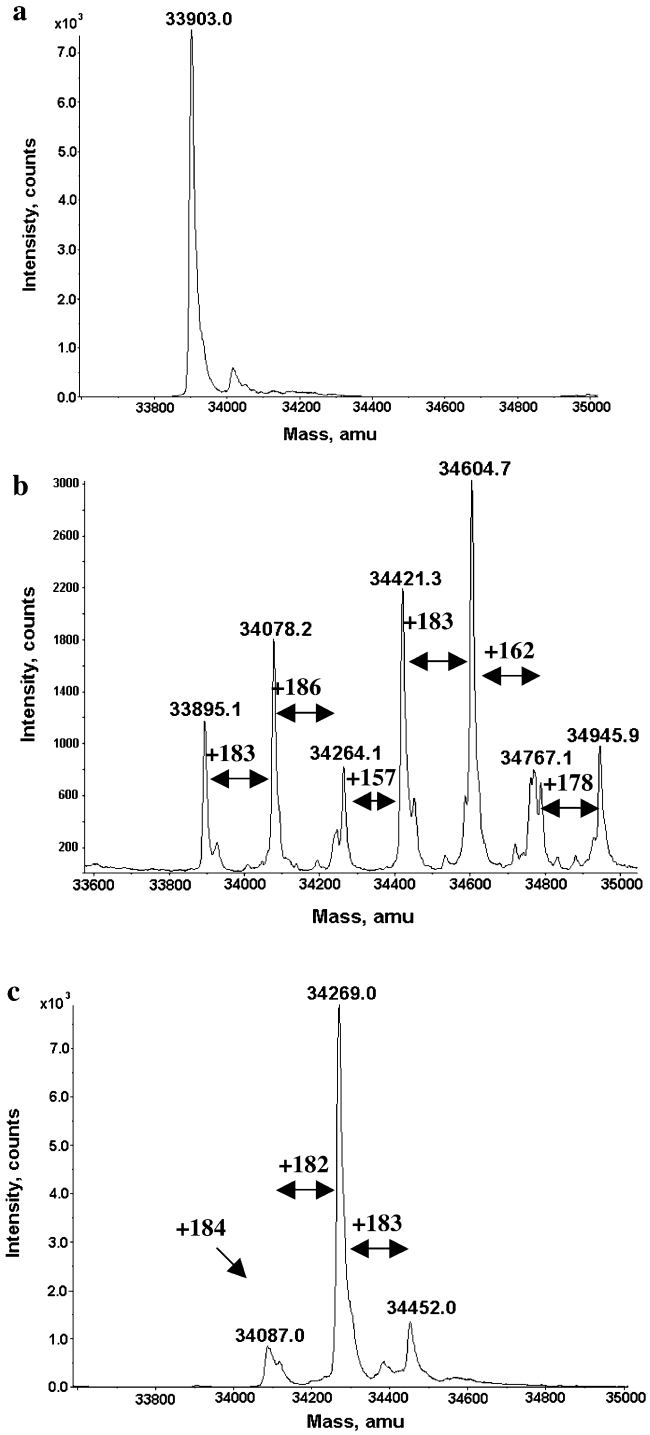

Figure 3. Deconvoluted ESI Q-TOF mass spectra: (a) native hamster NAT1, (b) N-OH-4-AABP-inactivated hamster NAT1, and (c) 4-nitrosobiphenyl-inactivated hamster NAT1.

sequence of DQIVRKKRGGWCLQVNHLLY. The presence of the b11 ion (1324.78, *m/z*) and the b12 ion (1459.76, *m/z*) is diagnostic for the +32 Da modification on Cys68, indicating that the thiol had been converted to a sulfinic acid (Figure 2b). Further evidence for the sulfinic acid modification arises from the fragment peaks at 1393.79 and 2392.38 Da, which match exactly with a neutral loss of H_2SO_2 (−66 Da) from the b12 ion (1459.76 *m/z*) and the y20 ion (2458.36 *m/z*), respectively. Because no peak showing a 32 Da mass shift was present in the control samples, it can be concluded that the sulfinic acid is the product of hydrolysis of a sulfinamide adduct and

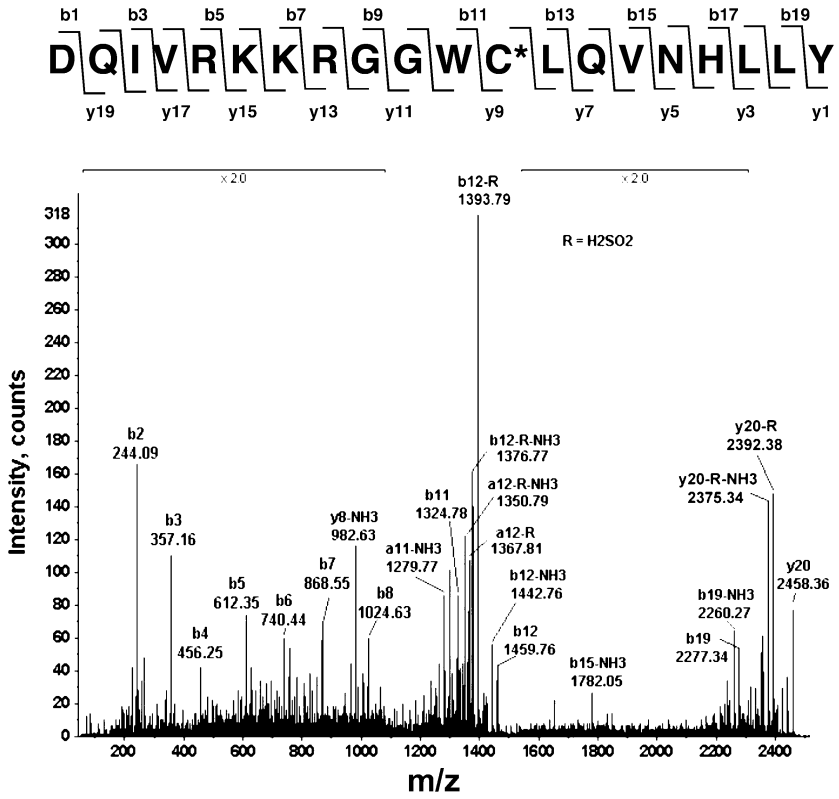

Figure 4. MALDI Q-TOF tandem mass spectrum of the 2458.31 Da peptide obtained by pepsin digestion of N-OH-4-AABP-inactivated hamster NAT1.

that the reactant responsible for the inactivation of hamster NAT1 is 4-nitrosobiphenyl (*17*).

To identify additional adducted amino acid residues, hamster NAT1 that had been inactivated by N-OH-4-AABP was subjected to treatment with trypsin, endoproteinase Glu-C, and a combination of the two proteases. One modified peptide with monoisotopic mass of 1591.3 Da was found in the endoproteinase Glu-C digests, which corresponds to the modified (+167 Da) sequence RIGYNNPVYTLD (Arg9−Asp20; unmodified theoretical mass, 1424.72 Da) (Supporting Information, Figure S2). The tandem MS data for the adducted peptide are shown in Figure 5. The a8 ion (886.45, *m/z*) and a9-NH_3 ion (1199.60, *m/z*) are diagnostic for the covalent conjugation of Tyr17 with 4-ABP. Additionally, a fragment peak at 303.14 *m/z*, which is 167 Da greater than the theoretical immonium ion for Tyr17 ($^+H_2N{=}CHCH_2PhOH$), allowed the unequivocal designation of Tyr17 as being covalently modified by 4-ABP.

The remaining four adducts that appear to be present in the mass spectrum of N-OH-4-AABP-modified hamster NAT1 (Figure 3b) could not be identified, even though the proteolytic digestions with pepsin, trypsin, and endoproteinase Glu-C afforded almost complete coverage of the sequence of hamster NAT1. Although three of the unidentified apparent adducts (∼183 Da) could have been generated by the reaction of 4-nitrosobiphenyl with cysteine thiols, none of the five cysteines of hamster NAT1, other than Cys68, was found to be modified.

ESI Q-TOF MS Analysis, Proteolysis, and MALDI Q-TOF MS/MS Analysis of N-OH-4-AABP-Treated Hamster NAT2. Native (untreated) hamster NAT2 exhibited a molecular mass of 34232.6, which matches the theoretical mass of 34233.1 Da, including the four additional amino acids (Gly, Thr, Leu, and Glu) at the N terminus of the recombinant protein (Figure 6a). Hamster NAT2 that had been treated with N-OH-4-AABP yielded a mass spectrum that contained three peaks (Figure 6b), the most intense of which (34232.0 Da) corresponds to unmodified hamster NAT2, whereas the peak of second greatest intensity (34415.2 Da) shows a mass increase of 183 Da, indicating either a semimercaptal or a sulfinamide adduct. The minor peak in Figure 6b (34574.5 Da) corresponds to a mass increase of 159 Da, relative to the 34415.2 Da peak.

To characterize the adducted amino acid residues, the N-OH-4-AABP-inactivated hamster NAT2 was treated with pepsin and the resulting digest was analyzed by MALDI Q-TOF MS. One modified (+32 Da) peptide of 2457.9 Da, corresponding to the sequence DQIVRKKRGGWCLQVNHLLY (Asp57−Tyr76; unmodified theoretical mass 2426.31 Da), was identified by comparing the spectrum with that of the control digest (Supporting Information, Figure S3). MALDI Q-TOF MS/MS analysis of the modified sequence allowed the assignment of Cys68 as the modified (+32 Da) residue, with the b11 ion (1324.74 *m/z*), the b12 ion (1459.76 *m/z*), and the very intense b12-H_2SO_2 ion (1393.76 Da) being diagnostic for the added mass of +32 Da, indicating that the thiol of Cys68 had been converted to a sulfinic acid (Figure 7).

Hamster NAT2 that had been inactivated with N-OH-4-AABP was also subjected to treatment with endopeptidase Glu-C. MALDI Q-TOF MS comparison of the resulting digest with a control digest identified a new peak of 1546.8 Da, which corresponds to the modified (+167 Da) sequence TWYLDQIRRE (Tyr158−Glu167, unmodified theoretical mass, 1378.70 Da) (Supporting Information, Figure S4). The tandem MS data for the adducted peptide are shown in Figure S5 (Supporting Information). The b2 ion (288.12 *m/z*), b3 ion (618.24 *m/z*),

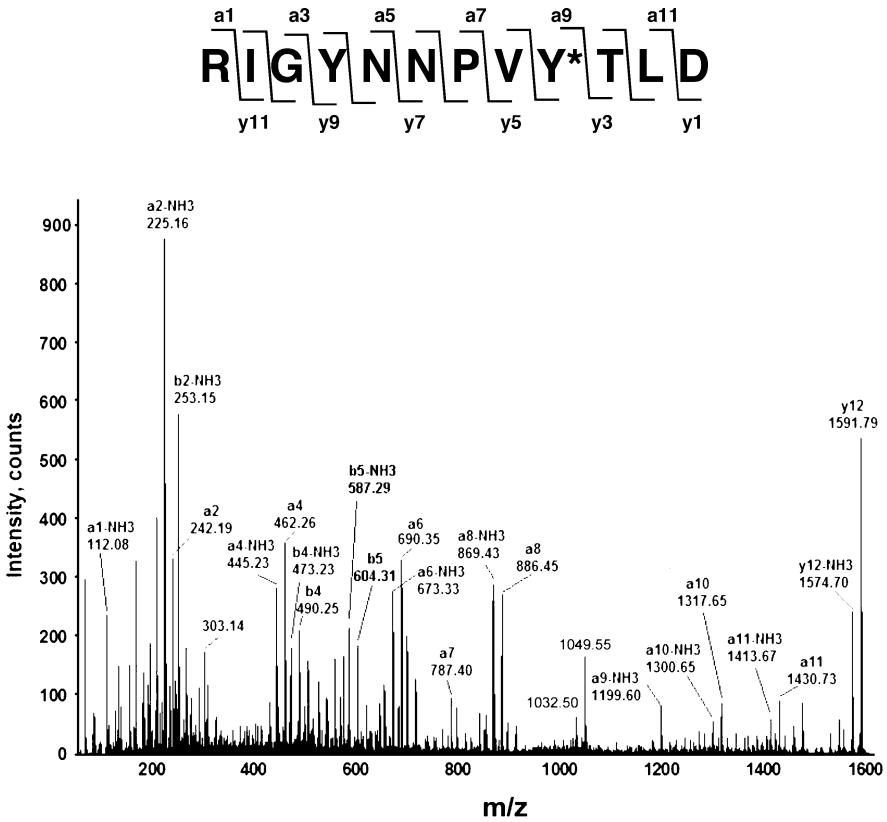

Figure 5. MALDI Q-TOF tandem mass spectrum of the 1591.3 Da peptide obtained by endoproteinase Glu-C-catalyzed digestion of N-OH-4-AABP-treated hamster NAT1.

and the characteristic immonium ion (303.13 *m/z*) generated by a modified Tyr are diagnostic and verify that Tyr160 is covalently bound to 4-ABP.

The mass spectra of both hamster NAT1 and hamster NAT2 that had been inactivated by N-OH-4-AABP contained minor peaks with adducts of +157 and +159 Da, respectively (Figures 3b and 6b). MALDI Q-TOF analysis of the digested protein samples, however, revealed only +167 Da adducts in addition to the sulfinamide (+183 Da) adducts. Apparently, the identified 4-ABP adducts (+167 Da) correspond to the mass increments of +157 and +159 Da seen in the modified protein mass spectra.

ESI Q-TOF MS Analysis, Proteolysis, and MALDI Q-TOF MS/MS Analysis of N-OH-4-AABP-Treated Human NAT1. The mass spectrum of native human NAT1 contains a peak of molecular mass 34296.7 Da, which corresponds to the theoretical mass of 34299.2 Da, including the four additional residues (Gly, Thr, Leu, and Glu) that are present at the N terminus of the recombinant protein (Figure 8a). Human NAT1 that had been treated with N-OH-4-AABP exhibited a single major peak of 34479.1 Da, corresponding to a mass increment of 179 Da relative to the 34299.8 Da peak for unmodifed human NAT1 (Figure 8b). Two minor, but significant, peaks appear at 34646.1 and 34664.6 Da, corresponding to mass increases of 167 and 185 Da, respectively, relative to the 34479.1 Da peak (Figure 8b). The peaks with mass shifts of +179 and +185 Da can be interpreted as resulting from 4-nitrosobiphenyl adductions, and the 167 Da mass enhancement can be attributed to a 4-ABP adduct.

The N-OH-4-AABP-modified human NAT1 was subjected to pepsin digestion, and the digested sample was analyzed by MALDI Q-TOF MS. Three modifed peptides were revealed with monoisotopic masses of 1590.78, 1613.80, and 1715.60 Da and were not present in the pepsin digest of native human NAT1 (Supporting Information, Figure S6). MALDI Q-TOF MS/MS analysis of the peptide of mass 1590.78 Da identified the modified (+32 Da) sequence DQVVRRNRGGWCL (Asp57−Leu76; unmodified theoretical mass 1558.78 Da). The b11-NH_3 ion (1307.63 *m/z*), b12 ion (1459.64 *m/z*), and the intense b12-H_2SO_2 ion (1393.67 *m/z*) are diagnostic for the added mass of +32 Da, indicating that the thiol of Cys68 had been converted to a sulfinic acid (Figure 9).

Tandem MS analysis of the peptide of mass 1613.80 Da identified the modified (+167 Da) sequence IRREQYIPNEE (Ile164−Glu174, unmodified theoretical mass 1446.58 Da). The a5 ion (655.36 *m/z*), b5-NH_3 ion (666.37 *m/z*), a6-NH_3 (968.49 *m/z*), b6-NH_3 ion (996.40 *m/z*), and the immonium ion (303.14 *m/z*) produced from the modified Tyr unequivocally identify Tyr169 as the 4-ABP modified residue (Supporting Information, Figure S7). Tandem MS analysis of the peptide of mass 1715.60 Da revealed the modified (+167 Da) sequence LEDSKYRKIYSF (Leu181−Phe192, unmodified theoretical mass 1548.76 Da). The b5-H_2O ion (555.25 *m/z*), b6-H_2O ion (885.42*m/z*), and the immonium ion (303.13 *m/z*) are distinctly diagnostic for the designation of Tyr186 as the 4-ABP-derivatized residue (Supporting Information, Figure S8).

ESI Q-TOF MS Analysis, Proteolysis, and MALDI Q-TOF MS/MS Analysis of 4-Nitrosobiphenyl-Treated Hamster NAT1, Hamster NAT2, and Human NAT1. The results described above indicate that the Cys68 adduct formed upon treatment of the NATs with N-OH-4-AABP is the result of a reaction with 4-nitrosobiphenyl. Thus, 4-nitrosobiphenyl was synthesized and

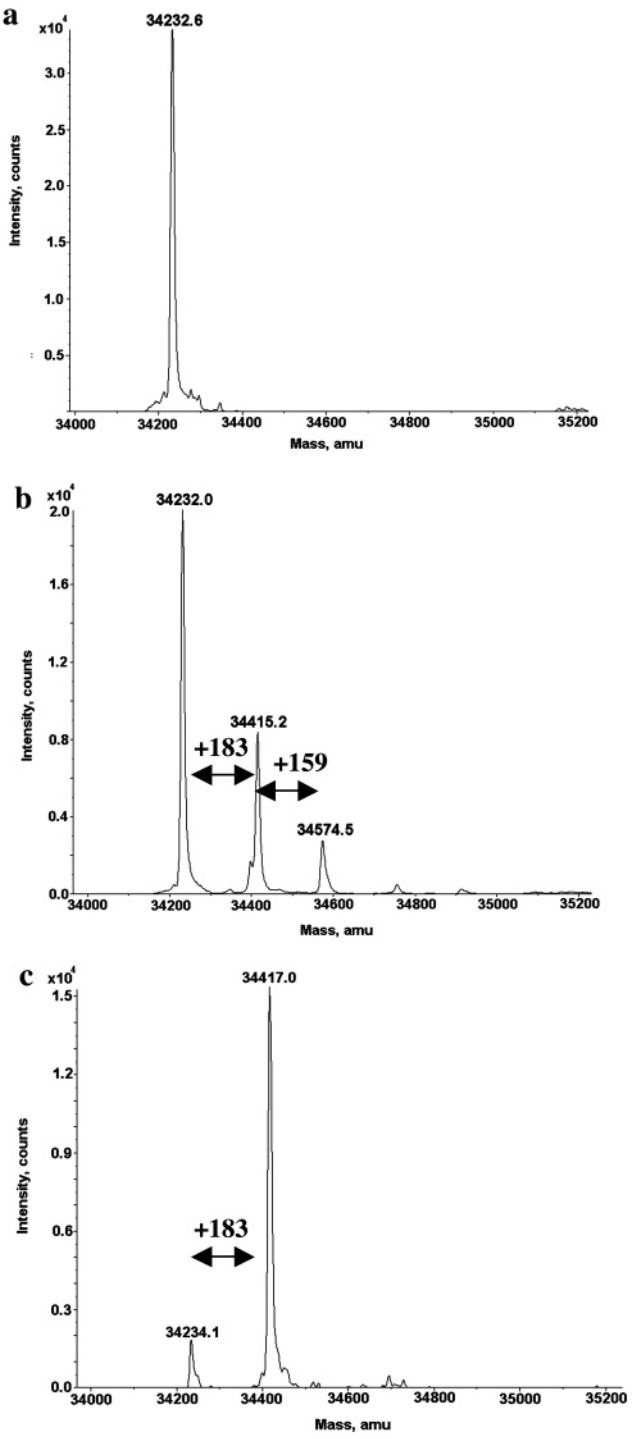

Figure 6. Deconvoluted ESI Q-TOF mass spectra: (a) native hamster NAT2, (b) N-OH-4-AABP-inactivated hamster NAT2, and (c) 4-nitrosobiphenyl-inactivated hamster NAT2.

the products of its reaction with the three NATs were identified. The ESI Q-TOF mass spectrum of 4-nitrosobiphenyl-treated hamster NAT1 exhibited a minor peak at 34087.0 Da, a major peak at 34269.0 Da, and another minor peak at 34452.0 Da, corresponding to an average 183 ± 1 Da mass increment relative to the native protein mass, to the 34087.0 Da peak and to the 34269.0 Da peak, respectively (Figure 3c). The ESI Q-TOF mass spectrum of 4-nitrosobiphenyl-treated hamster NAT2 exhibited a small peak (34234.1 Da), which corresponds to the native protein mass, and a major peak (34417.0 Da), indicating the addition of a single 4-nitrosobiphenyl molecule (+183 Da) (Figure 6c). As shown in Figure 8c, the 4-nitrosobiphenyl-treated human NAT1 exhibits one major peak (34479.3 Da), which corresponds to a 182 Da mass increase relative to the peak (34297.4 Da) for the native protein. Thus, each NAT contained one or more modifications corresponding to covalent addition of 4-nitrosobiphenyl (+183 Da), but no 4-ABP adducts (+167 Da) were present.

Each of the 4-nitrosobiphenyl-modified NATs was subjected to pepsin digestion, and the resulting digests were analyzed by MALDI-Q-TOF MS. For hamster NAT1, only one modified peptide (+32 Da) with a monoisotopic mass of 2458.51 Da, corresponding to the sequence DQIVRKKRGGWCLQVNHLLY (Asp57−Tyr76; unmodified theoretical mass, 2426.32 Da), was identified (Supporting Information, Figure S1). MALDI Q-TOF MS/MS analysis of the modified sequence allowed the assignment of Cys68 as the modified (+32 Da) residue, with the b11 ion (1324.78 *m/z*), b12 ion (1459.76 *m/z*), and b12-H_2SO_2 ion (1393.79 Da) being diagnostic for the added mass of 32 Da, and indicating that the thiol of Cys68 had been converted to a sulfinic acid (Supporting Information, Figure S9).

MALDI Q-TOF MS analysis of pepsin-digested hamster NAT2 that had been incubated with 4-nitrosobiphenyl revealed one modified peptide (+32 Da) with a monoisotopic mass of 2458.61 Da, corresponding to the sequence DQIVRKKRGGWCLQVNHLLY (Asp57−Tyr76; unmodified theoretical mass, 2426.32 Da) (Supporting Information, Figure S3). The rpHPLC fraction containing the modified peptide was treated with endopeptidase Lys-C, which produced the modified (+32 Da) peptide of mass 1590.90 Da, corresponding to the sequence RGGW-CLQVNHLLY (Arg64−Tyr76). The tandem MS data for the latter peptide are shown in the Supporting Information (Figure S10). The b4 ion (457.2 *m/z*), b5 ion (592.2 *m/z*), and b5-H_2SO_2 ion (526.2 *m/z*) verify that Cys68 had been modified by 4-nitrosobiphenyl to form a sulfinamide, followed by hydrolysis to yield a sulfinic acid adduct.

MALDI Q-TOF MS analysis of pepsin-digested human NAT1 that had been incubated with 4-nitrosobiphenyl revealed one modified (+32 Da) peptide of mass 1590.78 Da (Supporting Information, Figure S11). MALDI Q-TOF MS/MS identified the modified (+32 Da) sequence DQV-VRRNRGGWCL (Asp57−Leu76; unmodified theoretical mass 1558.78 Da). The b11-NH_3 ion (1307.63 *m/z*), b12 ion (1459.64 *m/z*), and the intense b12-H_2SO_2 ion (1393.67 *m/z*) are diagnostic for the added mass of +32 Da, indicating that the thiol of Cys68 had been converted to a sulfinic acid (Supporting Information, Figure S12).

Formation of 4-Nitrosobiphenyl from N-OH-4-AABP During Incubation with NATs. The data shown in Figure 1 indicate distinct kinetic differences in the inactivation of the three NATs by N-OH-4-AABP. In particular, hamster NAT2 and human NAT1 inactivation are characterized by a delay in the onset of diminished activity. Therefore, experiments were conducted to determine whether differences in the rates of generation of the inactivating reactant, 4-nitrosobiphenyl, could be detected. Each of the NATs (4 μM) was incubated with N-OH-4-AABP (200 μM), and the characteristic 4-nitrosobiphenyl absorbance at 350 nm was monitored continuously for 30 min (Figure 10). The reaction between human NAT1 and N-OH-4-AABP resulted in a continu-

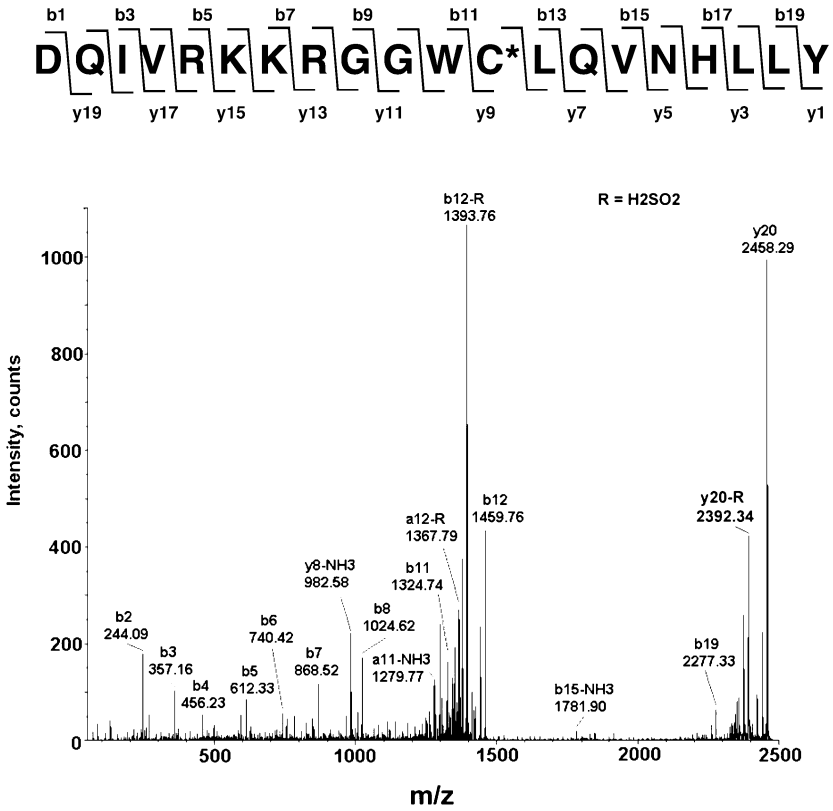

Figure 7. MALDI Q-TOF tandem mass spectrum of the 2457.9 Da peptide obtained by pepsin digestion of N-OH-4-AABP-inactivated hamster NAT2.

ous increase in absorbance to a maximum of 0.21 units after 30 min, which corresponds to a 4-nitrosobiphenyl concentration of approximately 20 μM. Similarly, the catalytic transformation of N-OH-4-AABP by hamster NAT2 yielded approximately 10 μM 4-nitrosobiphenyl, whereas the incubation of hamster NAT1 with N-OH-4-AABP caused an absorbance increment of only 0.02 units, corresponding to 2 μM 4-nitrosobiphenyl. The latter increase in absorbance was measurable within the first 2 min of incubation, and there was no detectable increase thereafter. Thus, hamster NAT1, which of the three NATs studied is the most efficiently inactivated in the presence of N-OH-4-AABP, generates relatively little detectable 4-nitrosobiphenyl. Human NAT1 and hamster NAT2, however, are inactivated less rapidly than hamster NAT1 in the presence of N-OH-4-AABP but produce substantially greater quantities of the nitroso product.

Half-Lives of the Acetylated NATs. On the basis of results obtained with N-OH-AAF, it is expected that inactivation of NATs in the presence of N-arylhydroxamic acids, such as N-OH-4-AABP, involves initial enzyme-mediated deacetylation to generate N-OH-4-ABP and an NAT in which the Cys68 residue is acetylated (*17*). The acetyl group must be removed before the side chain thiol of Cys68 is available to react with 4-nitrosobiphenyl, which is the oxidation product of N-OH-4-ABP. To compare the hydrolytic stabilities of the acetylated enzymes, each NAT was incubated with PNPA, and the rates of 4-nitrophenol formation were determined by monitoring its absorbance at 400 nm. With each enzyme, the production of 4-nitrophenol proceeded at a constant rate, following an initial burst. The steady state rates, calculated from the slopes of the lines, were 10^4 lower than those observed in the specific activity assays when either PABA or anisidine was the acetyl acceptor, indicating that acetyl−enzyme hydrolysis is rate limiting. Therefore, the steady state rate constants represent the rate constants for hydrolysis of the acetyl−enzyme (k_{H_2O}), from which the half-lives of the acetyl−enzymes ($t_{1/2} = 0.693/k_{H_2O}$) were calculated (Table 1). The half-life of each acetyl−enzyme was approximately 2-fold longer at 25 °C than at 37 °C. More significantly, acetylated hamster NAT1 has a half-life of 4.7 s at 37 °C, which is 8-fold less than the half-life of acetylated hamster NAT2 and 7-fold less than that of acetylated human NAT1 (Table 1). Thus, the two NATs, hamster NAT2 and human NAT1, which exhibit measurable delays in undergoing inactivation after exposure to N-OH-4-AABP, form thiol ester intermediates that are substantially more stable than that of the more rapidly inactivated hamster NAT1.

Inactivation of Hamster NAT1, Hamster NAT2, and Human NAT1 by 4-Nitrosobiphenyl. To evaluate the relative sensitivities of the three NATs to inactivation by 4-nitrosobiphenyl, a preliminary concentration−effect study was conducted. Incubations were carried out with each of the NATs (0.73 μM) and three concentrations of 4-nitrosobiphenyl (1, 5, and 10 μM), corresponding to inactivator:enzyme ratios of 1.3:1, 6.5:1, and 13:1. Because hamster NAT1 is rapidly inactivated by 4-nitrosobiphenyl, the incubations were conducted at 23 °C to permit detection of differences in the sensitivity of the NATs to the reagent. The lowest concentration of 4-nitrosobiphenyl (1 μM) caused a 44% loss of hamster NAT1 activity during 1 min of exposure, but the activities of hamster NAT2 and human NAT1 were reduced by only 12−13% (Figure 11). The higher concentrations of 4-nitrosobiphenyl caused further losses of activity by all three NATs, but hamster NAT1 exhibited the greatest extent of inactivation.

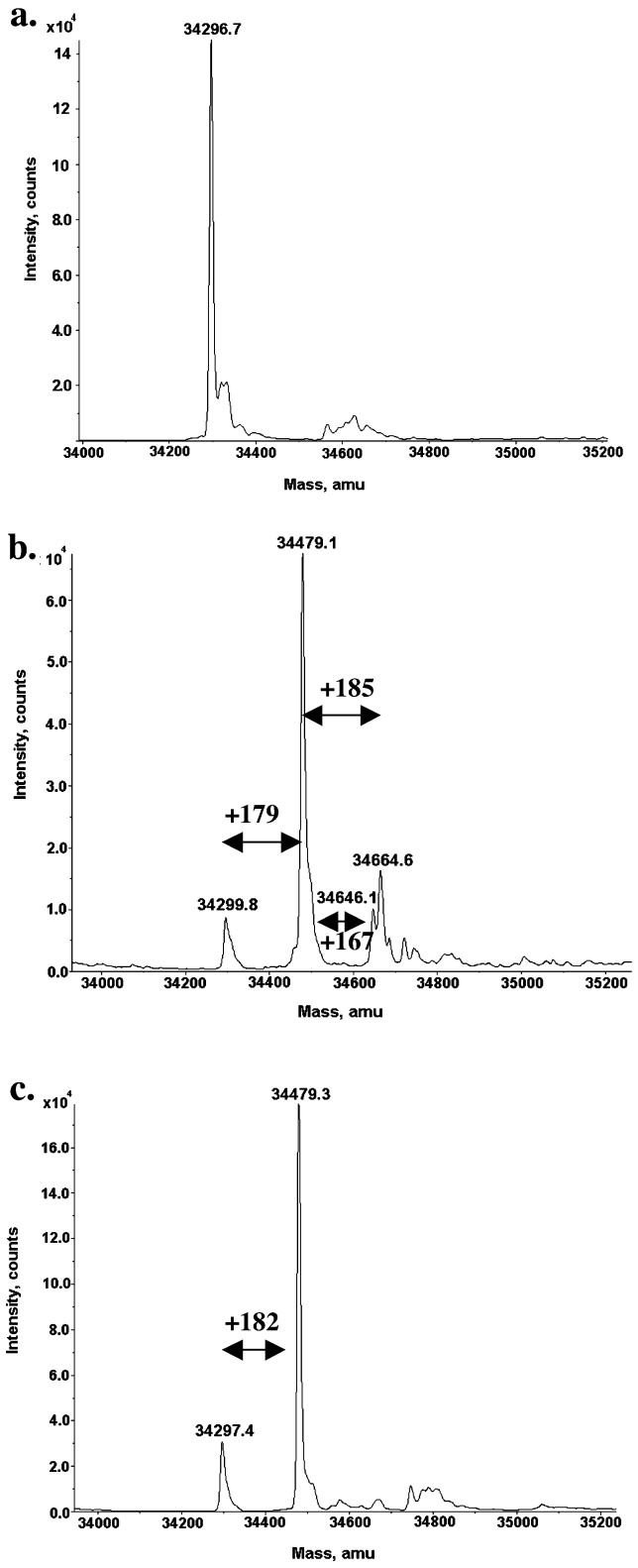

Figure 8. Deconvoluted ESI Q-TOF mass spectra: (a) native human NAT1, (b) N-OH-4-AABP-inactivated human NAT1, and (c) 4-nitrosobiphenyl-inactivated human NAT1.

Discussion

Evidence that the cofactor-independent conversion of carcinogenic N-arylhydroxamic acids to electrophilic reactants in mammalian cell cytosols involves the formation of reactive N-acetoxyarylamines was reported in 1972 (*36*). Subsequently, it was established that the cytosolic transformation of N-arylhydroxamic acids to N-acetoxyarylamines via N,O-acyl transfer is catalyzed by NATs (*37*). We found that both hamster NAT1 and NAT2 undergo pseudo-first-order, self-catalyzed irreversible inactivation in the presence of N-OH-AAF and, more recently, we determined that the reactive product responsible for the inactivation of hamster NAT1 by N-OH-AAF is 2-nitrosofluorene (*17*, *20*, *21*). Nitrosoarenes are electrophilic compounds that form sulfinamides upon reaction with nucleophilic thiols (*38*). Sulfinamide adduct formation with protein thiols may have toxicological significance. Nitroso derivatives of sulfonamide drugs form protein adducts, and nitrosoarenes have been shown to inactivate an aryl sulfotransferase in vitro (*39*−*41*). The finding that incubation with N-arylhydroxylamines causes irreversible inactivation of human NAT1, both in cultured cells and in cell cytosols, is consistent with adduction by nitrosoarenes, formed as oxidation products of the hydroxylamines (*42*).

ESI Q-TOF mass spectrometric analysis of hamster NAT1, hamster NAT2, and human NAT1, after incubation with N-OH-4-AABP, revealed that for each enzyme the major adduct caused a mass increment of 180−183 Da, which is consistent with a reaction having occurred between 4-nitrosobiphenyl and a cysteine thiol group to produce a (4-biphenyl)sulfinamide (Figure 2a). This result is identical with that observed for the inactivation of hamster NAT1 by N-OH-AAF, in that the predominant protein modification in both instances was a sulfinamide, which had been formed by reaction of a nitrosoarene with a cysteine thiol (*17*). Also similar to the results obtained with hamster NAT1 and N-OH-AAF was that treatment of hamster NAT1, hamster NAT2, and human NAT1 with N-OH-4-AABP, followed by proteolysis and tandem mass spectrometric analysis, resulted in identification of a sulfinic acid modification of the catalytically essential Cys68 (Figure 2b). Thus, the initially formed sulfinamide, which is responsible for irreversible inactivation of the NATs, undergoes hydrolysis to a sulfinic acid during proteolysis and sample preparation for MS/MS analysis. The conclusion that the Cys68 modifications observed after incubation of the three NATs with N-OH-4-AABP were the result of reactions with 4-nitrosobiphenyl was confirmed by the finding that identical Cys68 adducts were produced by treatment of the enzymes with either N-OH-4-AABP or 4-nitrosobiphenyl.

The bioactivation of carcinogenic N-arylhydroxamic acids by NATs results in the production of N-acetoxyarylamines, such as N-OAc-4-ABP (Scheme 1), which yield N-arylnitrenium ions following heterolysis of the N−O bond. The current consensus is that N-arylnitrenium ions are the primary reactants responsible for arylamine−DNA adduct formation, although the possibility that certain highly electronegative N-acetoxyarylamines may initially form arylnitrenes has been suggested (*14*−*16*, *43*−*46*). The treatment of hamster NAT1, hamster NAT2, and human NAT1 with N-OH-4-AABP afforded minor quantities of 4-ABP−tyrosine adducts. Although 4-ABP adducts are the expected products of nitrenium ion intermediates, further studies are required to elucidate their specific mechanism of formation.

The inactivation of hamster NAT1 by the carcinogenic hydroxamic acid, N-OH-4-AABP, follows pseudo-first-order kinetics, although the enzyme was inactivated less efficiently by N-OH-4-AABP than by N-OH-AAF, as indicated by their respective k_i/K_I values of 63 and 364

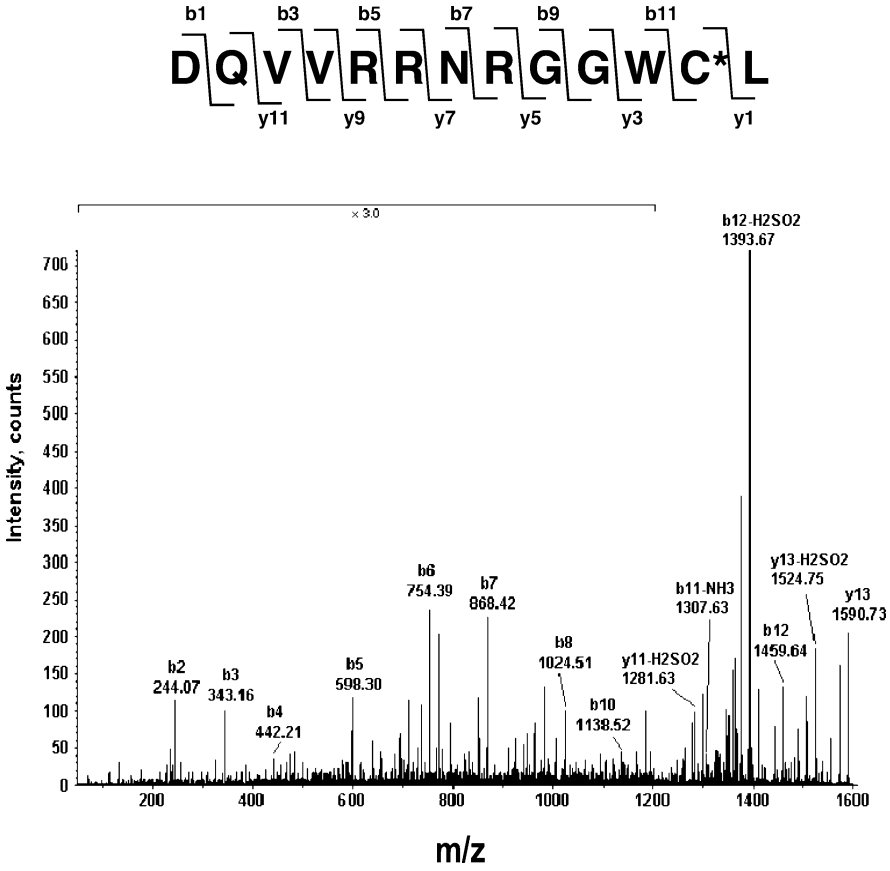

Figure 9. MALDI Q-TOF tandem mass spectrum of the 1590.78 Da peptide obtained by pepsin digestion of N-OH-4-AABP-inactivated human NAT1.

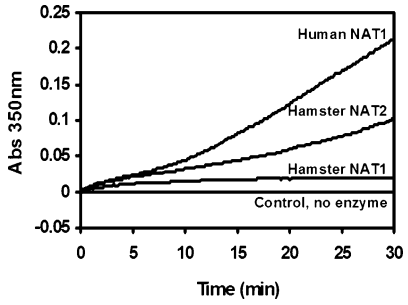

Figure 10. 4-Nitrosobiphenyl formation from N-OH-4-AABP (200 μM) in the presence of NATs (4 μM). The results represent the average of three independent experiments.

Table 1. Hydrolysis Rate (k_{H_2O}) and Half-Lives ($t_{1/2}$) of Acetylated NATs[a]

	37 °C		25 °C	
	k_{H_2O} (s^{-1})[b]	$t_{1/2}$ (s)	k_{H_2O} (s^{-1})	$t_{1/2}$ (s)
hamster NAT1	0.147 ± 0.003	4.7	0.072 ± 0.002	9.6
hamster NAT2	0.018 ± 0.002	39.4	0.008 ± 0.001	90.0
human NAT1	0.021 ± 0.001	32.7	0.011 ± 0.000	63.6

[a] Experiments were conducted as described in the Experimental Procedures. [b] Results are expressed as the means (± SD) of three experiments.

M^{-1} s^{-1} (*20*). In contrast to hamster NAT1, however, inactivation of hamster NAT2 by N-OH-4-AABP did not occur by a first-order process, and inactivation was observed only after a lag period of approximately 2 min following initial exposure of the enzyme to the hydroxamic acid. The inactivation of hamster NAT2 by N-OH-4-AABP took place at a faster rate at longer incubation times than in the early phases of incubation. The latter

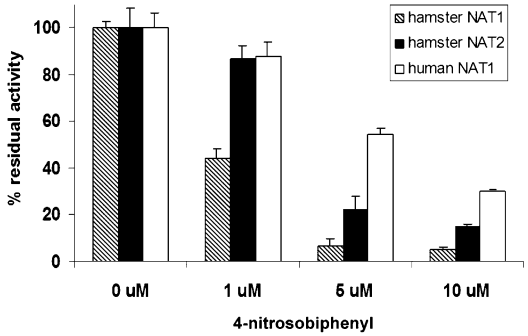

Figure 11. Effect of 4-nitrosobiphenyl on NAT activities. The incubations were carried out as described in the Experimental Procedures. The results represent the means of two experiments. At 1 μM, the results for hamster NAT1 are significantly different from those for hamster NAT2 and human NAT1 ($P < 0.01$). At 5 μM, the results for hamster NAT1 are different from those for hamster NAT2 ($P < 0.05$) and human NAT1 ($P < 0.01$), and the results for hamster NAT2 are different from those for human NAT1 ($P < 0.01$). At 10 μM, the results for hamster NAT1 are different from those for hamster NAT2 and human NAT1 ($P < 0.01$), and the results for hamster NAT2 are different from those for human NAT1 ($P < 0.01$).

kinetic results are similar to those observed for the inactivation of hamster NAT1 activity by the hydroxamic acid, N-hydroxy-N-(4-cyclohexylphenyl)acetamide, which were attributed to accumulation of an electrophilic product that subsequently reacts with the enzyme (*25*). Analogous to the results obtained with hamster NAT2, there was a delay of approximately 2 min after initiation of incubation with N-OH-4-AABP before loss of human NAT1 activity was detectable, although the inactivation of human NAT1 was a pseudo-first-order process.

Scheme 1

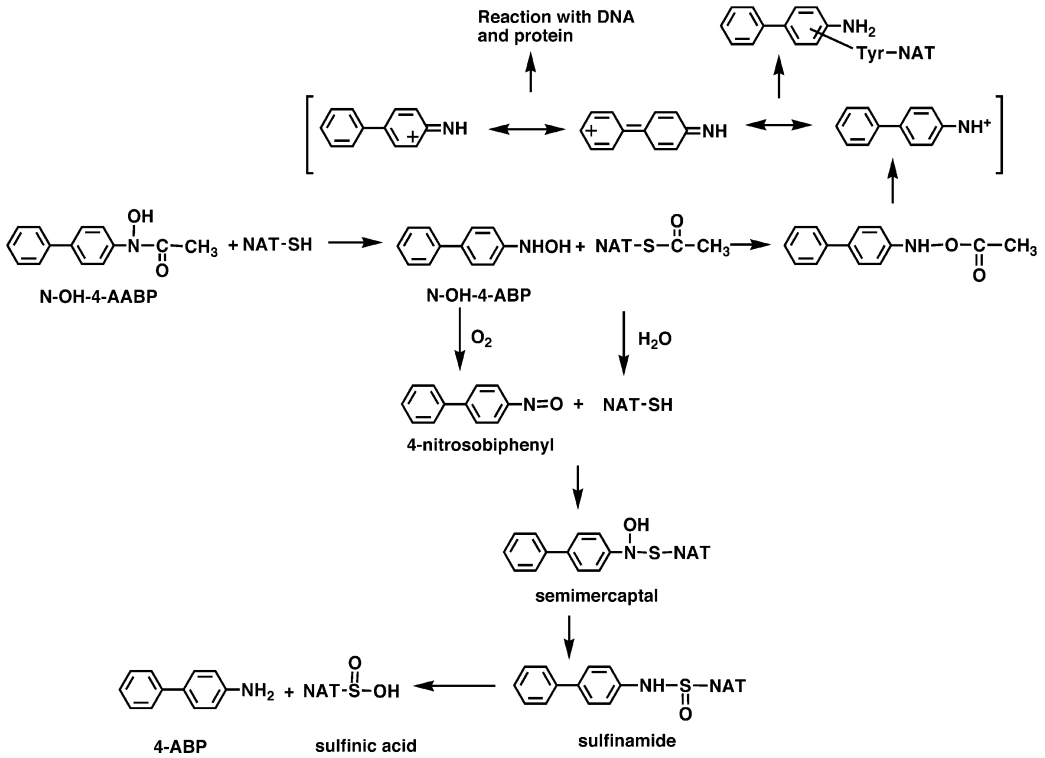

Because the lag period that occurs prior to inactivation of hamster NAT2 and human NAT1 by N-OH-4-AABP may indicate the accumulation of a reactive product in the incubation mixtures and because 4-nitrosobiphenyl was identified as the NAT-inactivating agent produced from N-OH-4-AABP, experiments were conducted to detect the presence of 4-nitrosobiphenyl in incubation mixtures containing N-OH-4-AABP and the three NAT isoforms. Treatment of human NAT1 and hamster NAT2 with N-OH-4-AABP resulted in production of 4-nitrosobiphenyl, which continuously increased in concentration during 30 min of incubation. This result supports the proposal that the delay in loss of activity by human NAT1 and hamster NAT2 upon incubation with N-OH-4-AABP coincides with the generation and accumulation of 4-nitrosobiphenyl.

A number of N-arylhydroxamic acids, such as N-OH-AAF and N-OH-4-AABP, function as acetyl donors for NATs, a process that yields an arylhydroxylamine and an acetylated NAT in which the acetyl group is retained on the Cys68 side chain as a thiol ester (Scheme 1). Oxidation of the arylhydroxylamine produces a nitrosoarene, which can react with the active site cysteine thiol (Cys68) to form a sulfinamide adduct (*17*). The reaction of the nitrosoarene with Cys68, however, cannot occur when the thiol group is acetylated. In the absence of an arylamine substrate to which the acetyl group can be transferred and under the conditions of the N-OH-4-AABP incubations with the NATs, the principal mode of deacetylation of the enzymes would be expected to be hydrolysis, along with a limited amount of N-acetylation and O-acetylation of the stoichiometric quantities of N-OH-4-ABP formed as a result of acetylation of the enzymes by the hydroxamic acid. Thus, it is reasonable to expect that the susceptibility to N-arylhydroxamic acid-mediated inactivation of NATs would be influenced by the relative stabilities of the acetyl−enzyme intermediates. Measurement of the rates of hydrolysis of the acetylated forms of the three NAT isozymes revealed the half-lives of acetylated hamster NAT2 and human NAT1 to be approximately 8- and 7-fold greater, respectively, than the half-life of acetylated hamster NAT1. This result is consistent with the observed accumulation of 4-nitrosobiphenyl during incubation of N-OH-4-AABP with hamster NAT2 and human NAT1 (Figure 10), and it may explain in part the previously observed selective inactivation of NAT1 in vivo after administration of N-OH-AAF to hamsters (*47*).

Hamster NAT1 is more readily inactivated by 4-nitrosobiphenyl than is either hamster NAT2 or human NAT1, as shown in Figure 11. Thus, both the relatively lower stability of the acetylated form of hamster NAT1 and its more facile inactivation by 4-nitrosobiphenyl appear to be factors that contribute to the kinetic differences in the irreversible loss of hamster NAT1, hamster NAT2, and human NAT1 activities in the presence of N-OH-4-AABP. Other processes that may influence the kinetic results but which are not accounted for by the present data are the comparative rates of acetylation of the NATs by N-OH-4-AABP, the rate of N-acetylation of N-OH-4-ABP to regenerate N-OH-4-AABP, and the rate of O-acetylation of N-OH-4-ABP to form N-OAc-4-ABP (Scheme 1). With regard to the capacities of NATs to utilize N-arylhydroxamic acids as acetyl donors, we have determined that the specific activity of human NAT1 in an assay with N-OH-AAF as the acetyl donor, and with AAB as the arylamine substrate, is 0.86 μmol/min/mg of protein. This value is comparable to that of hamster NAT2 (0.54 μmol/min/mg of protein) and is more than 20-fold lower than that of hamster NAT1 (*20*, *31*). These data suggest that of the three NATs evaluated in the present study, hamster NAT1 may exhibit the greatest capacity for catalysis of the deacetylation of N-arylhydroxamic acids, although additional experiments with other arylamine substrates are needed. The low level of human NAT1 activity in the

N-OH-AAF/AAB assay is intriguing because the capacity of human NAT1 for catalyzing the conversion of N-arylhydroxamic acids to reactive N-acetoxyarenes by N,O-acetyltransfer appears to be substantially greater than that of human NAT2, based on the relative rates of DNA adduct formation in the presence of the two enzymes (*19*). As shown in Scheme 1, N-acetoxyarene formation requires transfer of the acetyl group from the hydroxamic acid to NAT as an initial step.

Both our previously reported results and those presented herein demonstrate that irreversible inactivation of mammalian NATs in the presence of N-arylhydroxamic acids proceeds through reaction of a nitrosoarene with the catalytically essential Cys68 (*17*). Not only are there substantial differences in the susceptibility of NAT isoforms to self-catalyzed inactivation by N-arylhydroxamic acids, there are differences in their reactivity toward 4-nitrosobiphenyl. Thus, certain NATs may be specific targets for inactivation by nitrosoarenes, which are electrophilic oxidation products of numerous arylamines to which humans are exposed. The methodologies applied in the present research should be useful for identification of other protein targets of nitrosoarenes.

The substrate specificities of human NAT1 are similar to those of hamster NAT2 and, similarly, human NAT2 and hamster NAT1 prefer the same substrates (*19*, *48*, *49*). Hamster NAT1 is much more sensitive to N-OH-4-AABP-mediated inactivation than is either hamster NAT2 or human NAT1. This relative susceptibility to inactivation is consistent with the substrate selectivities of the three isoforms and fosters the expectation that human NAT2 will be similar to hamster NAT1 with regard to inactivation by N-arylhydroxamic acids and nitrosoarenes. Work is in progress to overexpress and purify human NAT2, which will be investigated for its propensity to undergo inactivation upon treatment with N-arylhydroxamic acids and nitrosoarenes.

Acknowledgment. We thank Drs. Thomas Krick, LeeAnn Higgins, and Sudha Marimanikkuppam of the Mass Spectrometry Consortium for the Life Sciences, University of Minnesota, for their advice and assistance. We thank Laura Silver for assistance with preparation of the manuscript. This research was supported in part by U.S. Public Health Service Grant CA55334 from the National Cancer Institute and by a Development Grant in Drug Design from the Department of Medicinal Chemistry, University of Minnesota.

Supporting Information Available: Segments of the MALDI-Q TOF mass spectra of protease digests of native, N-OH-4-AABP-inactivated and 4-nitrosobiphenyl-inactivated hamster NAT1, hamster NAT2, and human NAT1 (Figures S1−S4, S6, and S11). MALDI Q-TOF tandem mass spectra of peptides with 4-ABP-adducted tyrosine residues obtained by protease digestion of N-OH-4-AABP-inactivated hamster NAT2 and human NAT1 (Figures S5, S7, and S8). MALDI Q-TOF tandem mass spectra of peptides obtained by protease digestion of 4-nitrosobiphenyl-inactivated hamster NAT1, hamster NAT2, and human NAT1 (Figures S9, S10, and S12). Tables of theoretical and experimental *m/z* for ions from peptides obtained by protease digestion of N-OH-4-AABP-treated and 4-nitrosobiphenyl-treated hamster NAT1, hamster NAT2, and human NAT1 (Tables S1−S10).

References

(1) Yu, M. C., Skipper, P. L., Tannenbaum, S. R., Chan, K. K., and Ross, R. K. (2002) Arylamine exposures and bladder cancer risk. *Mutat. Res. 506−507*, 21−28.

(2) Vineis, P. (1994) Epidemiology of cancer from exposure to arylamines. *Environ. Health Perspect. 102* (S6), 7−10.

(3) Luceri, F., Pieraccini, G., Moneti, G., and Dolara, P. (1993) Primary aromatic amines from side-stream smoke are common contaminants of indoor air. *Toxicol. Ind. Health 9*, 405−413.

(4) Turesky, R. J., Freeman, J. P., Holland, R. D., Nestorick, D. M., Miller, D. W., Ratnasinghe, D. L., and Kadlubar, F. F. (2003) Identification of aminobiphenyl derivatives in commercial hair dyes. *Chem. Res. Toxicol. 16*, 1162−1173.

(5) Beland, F. A., and Kadlubar, F. F. (1990) Metabolic activation and DNA adducts of aromatic amines and nitroaromatic hydrocarbons. *Handbook Exp. Pharmacol. 94/I*, 267−325.

(6) Airoldi, L., Orsi, F., Magagnotti, C., Coda, R., Randone, D., Casetta, C., Peluso, M., Hautefeuille, A., Malaveille, C., and Vineis, P. (2002) Determinants of 4-aminobiphenyl-DNA adducts in bladder cancer. *Carcinogenesis 23*, 861−866.

(7) Faraglia, B., Chen, S. Y., Gammon, M. D., Zhang, Y. J., Teitelbaum, S. L., Neugut, A. I., Ahsan, H., Garbowski, G., Hibshoosh, H., Lin, D., Kadlubar, F. F., and Santella, R. M. (2003) Evaluation of 4-aminobiphenyl-DNA adducts in human breast cancer: The influence of tobacco smoke. *Carcinogenesis 24*, 719−725.

(8) Miller, J. A., Wyatt, C. S., Miller, E. C., and Hartmann, H. A. (1961) The N-hydroxylation of 4-acetylaminobiphenyl by the rat and dog and the strong carcinogenicity of N-hydroxy-4-acetylaminobiphenyl in the rat. *Cancer Res. 21*, 1465−1473.

(9) Enomoto, M., Lotlikhar, P., Miller, J. A., and Miller, E. C. (1962) Urinary metabolites of 2-acetylaminofluorene and related compounds in the rhesus monkey. *Cancer Res. 22*, 1336−1342.

(10) van de Poll, M. L. M., Venizelos, V., and Meerman, J. H. N. (1990) Sulfation dependent formation of N-acetylated and deacetylated DNA adducts of N-hydroxy-4-acetylaminobiphenyl in male rat liver in vivo and in isolated hepatocytes. *Carcinogenesis 11*, 1775−1781.

(11) Skipper, P. L., Obiedzinski, M. W., Tannenbaum, S. R., Miller, D. W., Mitchum, R. K., and Kadlubar, F. F. (1985) Identification of the major serum albumin adduct formed by 4-aminobiphenyl in vivo in rats. *Cancer Res. 45*, 5122−5127.

(12) King, C. M., Traub, N. R., Cardona, R. A., and Howard, R. B. (1976) Comparative adduct formation of 4-aminobiphenyl and 2-aminofluorene derivatives with macromolecules of isolated liver parenchymal cells. *Cancer Res. 36*, 2374−2381.

(13) Hanna, P. E. (1994) N-Acetyltransferases, O-acetyltransferases and N, O-acetyltransferases: Enzymology and bioactivation. *Adv. Pharmacol. 27*, 401−430.

(14) Kadlubar, F. F., and Beland, F. A. (1985) Chemical properties of ultimate carcinogenic metabolites of arylamines and arylamides. In *Polycylic Hydrocarbons and Carcinogenesis*, ACS Symposium Series 283 (Harvey, R. G., Ed.) pp 341−370, American Chemical Society, Washington, DC.

(15) Novak, M., and Rajagopal, S. (2002) Correlations of nitrenium ion selectivities with quantitative mutagenicity and carcinogenicity of the corresponding amines. *Chem. Res. Toxicol. 15*, 1495−1503.

(16) Kennedy, S. A., Novak, M., and Kolb, B. A. (1997) Reactions of ester derivatives of carcinogenic N-(4-biphenylyl)hydroxylamine and the corresponding hydroxamic acid with purine nucleosides. *J. Am. Chem. Soc. 119*, 7654−7664.

(17) Guo, Z., Wagner, C. R., and Hanna, P. E. (2004) Mass spectrometric investigation of the mechanism of inactivation of hamster arylamine N-acetyltransferase 1 by N-hydroxy-2-acetylaminofluorene. *Chem. Res. Toxicol. 17*, 275−286.

(18) Vatsis, K. P., Weber, W. W., Bell, D. A., Durpret, J.-M., Evans, D. A. P., Grant, D. M., Hein, D. W., Lin, H. J., Meyer, U. A., Relling, M. V., Sim, E., Suzuki, T., and Yamazoe, Y. (1995) Nomenclature for N-acetyltransferases. *Pharmacogenetics 5*, 1−17.

(19) Hein, D. W., Doll, M. A., Rustan, T. D., Gray, K., Feng, Y., Ferguson, R. J., and Grant, D. M. (1993) Metabolic activation and deactivation of arylamine carcinogens by recombinant human NAT1 and polymorphic NAT2 acetyltransferases. *Carcinogenesis 14*, 1633−1638.

(20) Sticha, K. R. K., Bergstrom, C. P., Wagner, C. R., and Hanna, P. E. (1998) Characterization of hamster recombinant monomorphic and polymorphic arylamine N-acetyltransferases. Bioactivation and mechanism based inactivation studies with N-hydroxy-2-acetylaminofluorene. *Biochem. Pharmacol. 56*, 47−59.

(21) Hanna, P. E., Banks, R. B., and Marhevka, V. C. (1982) Suicide inactivation of hamster hepatic arylhydroxamic acid N,O-acyltransferase. A selective probe of N-acetyltransferase multiplicity. *Mol. Pharmacol. 21*, 159−165.

(22) Kato, R., and Yamazoe, Y. (1995) Molecular mechanisms of polymorphism in acetylating enzymes for arylamines and N-hydroxyarylamines in hamster liver. *Drug Metab. Rev. 27*, 241−256.

(23) Hein, D. W., Doll, M. A., Fretland, A. J., Gray, K., Deitz, A. C., Feng, Y., Jiang, W., Rustan, T. D., Satran, S. L., and Wilkie, T. R., Sr. (1997) Rodent models of the human acetylatioin polymorphism: Comparisons of recombinant acetyltransferases. *Mutat. Res. 376*, 101−106.

(24) *NIH Guidelines for the Laboratory Use of Chemical Carcinogens* (1981) NIH Publication No. 81-2385, U.S. Government Printing Office, Washington, DC.

(25) Mangold, B. L., and Hanna, P. E. (1982) Arylhydroxamic acid N,O-acyltransferase substrates. Acetyl transfer and electrophile generating activity of N-hydroxy-N-(4-alkyl-, 4-alkenyl-, and 4-cyclohexylphenyl)acetamides. *J. Med. Chem. 25*, 630−638.

(26) Bradford, M. M. (1976) A rapid and sensitive method for the quantitation of microgram quantities of protein utilizing the principle of protein-dye binding. *Anal. Biochem. 75*, 248−254.

(27) Davey, M. H., Lee, V. Y., Miller, R. D., and Marks, T. J. (1999) Synthesis of aryl nitroso derivatives by *tert*-butyl hypochlorite oxidation in homogeneous media. Intermediates for the preparation of high-hyperpolarizability chromophore skeletons. *J. Org. Chem. 64*, 4976−4979.

(28) Westra, J. G. (1981) A rapid and simple synthesis of reactive metabolites of carcinogenic aromatic amines in high yield. *Carcinogenesis 2*, 355−357.

(29) Uehleke, H., and Nestel, K. (1967) Hydroxylaminobiphenyl and Nitrosobiphenyl: Biological oxidation products of 4-aminobiphenyl and reduction metabolites of 4-nitrobiphenyl. *Naunyn-Schmiedeberg's Arch. Pharmacol 257*, 157−171.

(30) Brill, E. (1974) The oxidation of some carcinogenic arylhydroxylamines to nitroso derivatives with manganese dioxide. *Experientia 30*, 835.

(31) Sticha, K. R. K., Sieg, C. A., Bergstrom, C. P., Hanna, P. E., and Wagner, C. R. (1997) Overexpression and large-scale purification of recombinant hamster polymorphic arylamine N-acetyltransferase as a dihydrofolate reductase fusion protein. *Protein Expression Purif. 10*, 147−153.

(32) Bergstrom, C. P., Wagner, C. R., Ann, D. K., and Hanna, P. E. (1995) Hamster monomorphic arylamine N-acetyltransferase: Expression in *Escherichia coli* and purification. *Protein Expression Purif. 6*, 45−55.

(33) Kitz, R., and Wilson, I. B. (1962) Esters of methanesulfonic acid as irreversible inhibitors of acetylcholinesterase. *J. Biol. Chem. 237*, 3245−3249.

(34) Guo, Z., Vath, G. M., Wagner, C. R., and Hanna, P. E. (2003) Arylamine N-acetyltransferases: Covalent modification and inactivation of hamster NAT1 by bromoacetamido derivatives of aniline and 2-aminofluorene. *J. Protein Chem. 22*, 631−642.

(35) Wang, H., Guo, Z., Vath, G. M., Wagner, C. R., and Hanna, P. E. (2004) Chemical modification of hamster arylamine N-acetyltransferase 2 with isozyme-selective and nonselective N-arylbromoacetamido reagents. *Protein J. 23*, 153−166.

(36) Bartsch, H., Dworkin, M., Miller, J. A., and Miller, E. C. (1972) Electrophilic N-acetoxyaminoarenes derived from carcinogenic N-hydroxy-N-acetylaminofluorenes by enzymatic deacetylation and transacetylation in liver. *Biochim. Biophys. Acta 286*, 272−298.

(37) Glowinski, I. B., Weber, W. W., Fysh, J. M., Vaught, J. B., and King, C. M. (1980) Evidence that arylhydroxamic acid N,O-acyltransferase and the genetically polymorphic N-acetyltransferase are properties of the same enzyme in rabbit liver. *J. Biol. Chem. 255*, 7883−7890.

(38) Kazanis, S., and McClelland, R. A. (1992) Electrophilic intermediate in the reaction of glutathione and nitrosoarenes. *J. Am. Chem. Soc. 114*, 3052−3059.

(39) Summan, M., and Cribb, A. E. (2002) Novel nonlabile covalent binding of sulfamethoxazole reactive metabolites to cultured human lymphoid cells. *Chem.-Biol. Interact. 142*, 155−173.

(40) Naisbitt, D. J., Farrell, J., Gordon, S. F., Maggs, J. L., Burkhart, C., Pichler, W. J., Pirmohamed, M., and Park, K. B. (2002) Covalent binding of the nitroso metabolite of sulfamethoxazole leads to toxicity and major histocompatibility complex-restricted antigen presentation. *Mol. Pharmacol. 62*, 628−637.

(41) King, R. S., and Duffel, M. W. (1997) Oxidation-dependent inactivation of aryl sulfotransferase IV by primary N-hydroxy arylamines during in vitro assays. *Carcinogenesis 18*, 843−849.

(42) Butcher, N. J., Ilett, K. F., and Minchin, R. F. (2000) Inactivation of human arylamine N-acetyltransferase 1 by hydroxylamine of p-aminobenzoic acid. *Biochem. Pharmacol. 60*, 1829−1836.

(43) Humphreys, W. G., Kadlubar, F. F., and Guengerich, F. P. (1992) Mechanism of C^8 alkylation of guanine residues by activated arylamines: Evidence for initial adduct formation at the N^7 position. *Proc. Natl. Acad. Sci. U.S.A. 89*, 8278−8282.

(44) Elfarra, A., and Hanna, P. E. (1985) Substituent effects on the bioactivation of 2-(N-hydroxyacetamido)fluorenes by N-arylhydroxamic acid N,O-acyltransferase. *J. Med. Chem. 28*, 1453−1460.

(45) Boteju, L. W., and Hanna, P. E. (1993) Bioactivation of N-hydroxy-2-acetylaminofluorenes by N,O-acyltransferase: Substituent effects on covalent binding to DNA. *Carcinogenesis 14*, 1651−1657.

(46) Boteju, L., and Hanna, P. E. (1994) Arylamine-nucleoside adduct formation: Evidence for arylnitrene involvement in the reactions of an N-acetoxyarylamine. *Chem. Res. Toxicol. 7*, 684−689.

(47) Smith, T. J., and Hanna, P. E. (1988) Hepatic N-acetyltransferases: Selective inactivation in vivo by a carcinogenic N-arylhydroxamic acid. *Biochem. Pharmacol. 37*, 427−434.

(48) Wagner, C. R., Bergstrom, C. P., Koning, K. R., and Hanna, P. E. (1996) Arylamine N-acetyltransferases. Expression in *Escherichia coli*, purification, and substrate specificities of recombinant hamster monomorphic and polymorphic isozymes. *Drug Metab. Dispos. 24*, 245−253.

(49) Levy, G. N., and Weber, W. W. (2002) Arylamine N-acetyltransferases. In *Enzyme Systems that Metabolize Drugs and Other Xenobiotics* (Ioaniddes, C., Ed.) pp 441−457, J. Wiley & Sons Ltd., New York.

TX049801W